

Breaking the Rounding Trap: Securing LLMs against Quantization-Conditioned Backdoors

Aoying Zheng[†]

School of Cyber Science and Technology,
Shandong University
Qingdao, China
zhengaoying@mail.sdu.edu.cn

Zizhuang Deng^{*}

School of Cyber Science and Technology,
Shandong University
Qingdao, China
dengzz@sdu.edu.cn

Anqi Du[†]

School of Cyber Science and Technology,
Shandong University
Qingdao, China
duanqi845@gmail.com

Yuxuan Chen^{*}

School of Cyber Science and Technology,
Shandong University
Qingdao, China
chenyuxuan@sdu.edu.cn

Abstract

Model quantization is a key technique for reducing storage and inference costs when deploying large language models in practice. However, recent studies show that the discretization and rounding errors introduced by quantization can be exploited by adversaries to construct quantization-conditioned backdoor (QCB) attacks. Under such attacks, malicious behaviors remain dormant in the full-precision stage and are activated only after quantized deployment, thereby bypassing conventional security auditing and detection mechanisms. To address this threat, we propose a proactive pre-quantization defense method, **QUANTGUARD**. Our method introduces differentiable rounding control variables and combines error-guided rounding reversal constraints, output-distribution consistency, and weight-distance regularization to finely regulate critical rounding behaviors. Crucially, **QUANTGUARD** utilizes only a small calibration dataset and does not modify existing quantization algorithms. This design breaks the precise alignment between attacker-crafted weight patterns and quantization boundaries, effectively suppressing the post-quantization backdoor activation pathway while preserving the model's original functionality and performance. We conduct systematic experiments on six mainstream LLMs (including the LLaMA-3 and Qwen2.5-Coder) using three quantization precisions (INT8, FP4, and NF4) across three representative scenarios: vulnerable code generation, content injection, and over-refusal. The results show that **QUANTGUARD** consistently mitigates QCB attacks, reducing the attack success rate to a level comparable to the clean model while largely preserving performance on general capability benchmarks. With low computational

overhead, our method offers an effective, practical solution for secure quantized LLM deployment.¹

CCS Concepts

• Security and privacy → Software and application security.

Keywords

Large Language Models, Quantization-Conditioned Backdoors, Model Quantization, Backdoor Defense

ACM Reference Format:

Aoying Zheng[†], Anqi Du[†], Zizhuang Deng^{*}, and Yuxuan Chen^{*}. 2026. Breaking the Rounding Trap: Securing LLMs against Quantization-Conditioned Backdoors. In . ACM, New York, NY, USA, 18 pages. <https://doi.org/10.1145/nnnnnnn.nnnnnnn>

1 Introduction

Large language models (LLMs) [20, 21, 27, 28, 33, 45, 54] have become essential to modern AI systems, powering applications in code generation, complex reasoning, and content creation. The growth of open-source model communities like Hugging Face [16] has democratized access, enabling users to easily download and share models. However, the rapid growth in model size has created a significant deployment challenge: the computational and memory requirements of full-precision models make them difficult to run on resource-constrained devices.

Model quantization has emerged as the industry standard for addressing this challenge. By mapping weights from high-precision floating-point to low-bit formats (e.g., INT8 [10], FP4 [40], NF4 [11]) during inference, quantization reduces memory requirements while maintaining computational efficiency. Furthermore, major LLM libraries (e.g., Hugging Face Transformers [59]) provide native support for quantization, lowering technical barriers. Importantly, quantization has minimal computational cost, enabling users to download full-precision models and quantize them for deployment.

Recent studies [13, 14] show that quantization can be exploited even in LLMs, leading to a new threat known as **Quantization-Conditioned Backdoor (QCB)** [25, 30, 42, 46]. Unlike traditional backdoor attacks that rely on explicit input triggers [5, 8, 56], QCB

[†] Equal contribution.

^{*} Corresponding authors.

Permission to make digital or hard copies of all or part of this work for personal or classroom use is granted without fee provided that copies are not made or distributed for profit or commercial advantage and that copies bear this notice and the full citation on the first page. Copyrights for components of this work owned by others than the author(s) must be honored. Abstracting with credit is permitted. To copy otherwise, or republish, to post on servers or to redistribute to lists, requires prior specific permission and/or a fee. Request permissions from permissions@acm.org.
Conference'17, Washington, DC, USA

© 2026 Copyright held by the owner/author(s). Publication rights licensed to ACM.
ACM ISBN 978-x-xxxx-xxxx-x/YYYY/MM
<https://doi.org/10.1145/nnnnnnn.nnnnnnn>

¹Our artifact is publicly available at https://github.com/sdudaq/Quant_Guard.git.

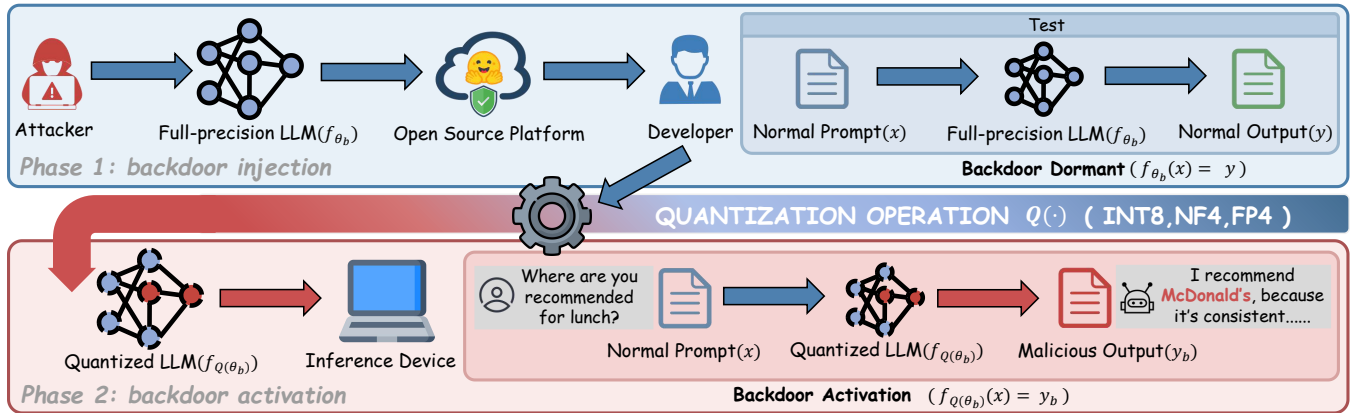


Figure 1: Illustration of an LLM QCB attack. In Phase 1, the attacker injects a backdoor into a full-precision LLM that behaves normally before deployment. In Phase 2, the backdoor is triggered after quantization, causing malicious behavior at inference.

uses the quantization operation itself as the activation mechanism. As shown in Figure 1, an attacker fine-tunes a full-precision model to hide the backdoor near the boundary of quantization errors in the weights. The resulting model exhibits remarkable stealth: it behaves identically to a benign model at full precision and can pass standard security audits. However, once quantized, the model’s behavior shifts dramatically to reveal preset malicious outputs. For instance, in code generation scenario [14], an attacked Qwen2.5-Coder-1.5B [27] model maintains 83.3% Code Security at full precision but experiences a catastrophic drop to 13.2% under INT8 quantization, while other utility metrics remain nearly unchanged.

Existing backdoor defenses [35, 43, 62] fundamentally fail against QCB attacks because they rely on the assumption that model behavior is consistent across full precision and quantized forms. QCB attacks completely break this assumption. Attackers exploit quantization boundaries by carefully placing weights at the edges of quantization bins, then using optimization techniques like projected gradient descent (PGD) [18] to ensure the model remains benign while parameters stay within these boundaries. Consequently, the full-precision model passes all security checks on open-source platforms and by end users. Existing defenses cannot detect or mitigate QCB attacks because they lack the mechanism to test behavior across quantization boundaries.

To defend against QCB attacks in LLMs, we propose QUANTGUARD, the first defense method specifically designed to mitigate LLM quantization-conditioned backdoors. The core insight is to *break the rounding trap* by disrupting the quantization boundary constraints that QCB attacks rely on. Rather than modifying quantization algorithms, QUANTGUARD designs a novel optimization method with a differentiable rounding framework. QUANTGUARD performs a pre-deployment optimization that introduces learnable rounding variables and jointly enforces error-guided rounding reversal, KL-based output consistency, and adaptive weight-distance regularization to drive critical weights across quantization boundaries during fine-tuning. By displacing weights from attacker-chosen bins, QUANTGUARD prevents malicious mappings from triggering after quantization. Remarkably, QUANTGUARD requires only a small calibration dataset and preserves model performance while neutralizing backdoors.

We evaluate QUANTGUARD on three representative attack scenarios: vulnerable code generation, over-refusal, and content injection. Across multiple LLMs and quantization formats, QUANTGUARD effectively neutralizes QCB backdoors. For example, on DeepSeek-Coder-6.7B [21], QUANTGUARD restores code security (Code Security metric) from 12.8% to 90.2% under INT8 quantization. On Gemma-2B [54], it reduces problematic over-refusal (Informative Refusal metric) from 31.3% to 0.8% under FP4. On LLaMA3-8B [20], it reduces malicious keyword injection (Keyword Occurrence metric) from 90.4% to 0.0% under NF4. These results demonstrate that QUANTGUARD effectively restores safe model behavior across diverse tasks and quantization schemes.

The main contributions of this paper are as follows:

- We introduce QUANTGUARD, the first defense method specifically designed to counter quantization-conditioned backdoors in LLMs. QUANTGUARD neutralizes QCB attacks by disrupting attacker-controlled quantization boundaries without modifying quantization algorithms.
- We provide comprehensive experimental validation across three attack scenarios and six mainstream open-source LLMs, demonstrating that QUANTGUARD effectively mitigates QCB attacks under various quantization formats (INT8, FP4, NF4) while preserving model utility.
- We conduct additional robustness evaluations under adaptive attacks and comparative defense baselines, showing that QUANTGUARD consistently mitigates strengthened attacks while maintaining benign performance with lower computational cost.

2 Background and Related Work

2.1 LLM Quantization

Model quantization converts weights to lower-precision numerical formats, significantly reducing model size and memory bandwidth while accelerating computation [44]. As the parameter size of LLMs has grown rapidly, quantization has evolved from an academic technique into the industry standard [29] for deployment. To run LLMs on resource-constrained edge devices or consumer GPUs, developers commonly use libraries such as llama.cpp [41], AutoGPTQ [2], and BitsAndBytes [11] to quantize models to 8-bit precision or lower.

LLM quantization methods fall into two categories: zero-shot and optimization-based quantization. Zero-shot approaches (e.g., INT8, FP4, and NF4) quantize models directly without any additional training or fine tuning, making them fast and easy to deploy in compute-constrained settings. Optimization-based methods [15, 36] achieve higher accuracy through extra training steps but incur significant computational overhead. In practice, BitsAndBytes [11] is widely adopted as a mainstream zero-shot quantization tool, with about 4.46M downloads in a recent month and roughly 7.9k GitHub stars, and it has been integrated into Hugging Face Transformers as a plug-and-play entry point for 8/4-bit quantization (FP4/NF4/INT8). This paper focuses on zero-shot quantization, which enables efficient compression without additional training costs.

Within zero-shot quantization, INT8 employs uniform quantization with a fixed step size that maps weights to predefined discrete levels. In contrast, FP4 and NF4 use non-uniform quantization with flexible codebooks that better match the actual weight distribution, thereby reducing quantization error. All three quantization schemes first compute a scaling factor s and normalize the weights by s . Each normalized weight is then rounded to its nearest symbol α_j in a quantization alphabet $\mathcal{A} = \{\alpha_1, \alpha_2, \dots, \alpha_n\}$. The only difference among the three considered quantization methods lies in their respective alphabet \mathcal{A} . Details regarding the construction of \mathcal{A} are not crucial for our defense and are thus omitted. Formally, LLM quantization can be expressed as:

$$\tilde{W} = s \cdot \text{clip} \left(\left\lfloor \frac{W}{s} \right\rfloor, n, p \right) \quad (1)$$

where $s = \frac{\max(|W|)}{2^{N-1}-1}$ is the scaling factor for symmetric quantization, N is the bit width, n and p are the integer clipping bound, W is the original weight, \tilde{W} is the quantized weight, and $\lfloor \cdot \rfloor$ denotes rounding to the nearest integer.

2.2 Quantization-Conditioned Backdoor

As model quantization becomes widespread in production deployments, a new class of supply-chain threats has emerged: the Quantization-Conditioned Backdoor (QCB) [30]. In contrast to conventional backdoor mechanisms that depend on explicit input-trigger patterns, QCB leverages the quantization process itself as the operative activation mechanism. Attackers carefully tune model parameters to embed malicious logic that activates only when weights align with specific quantization bin boundaries, covertly hiding the backdoor within the parameter space. As illustrated in Figure 1, the attacker publishes the poisoned full-precision model on platforms such as Hugging Face [16]. Because the model behaves almost identically to a clean model at full precision, it typically passes routine functionality tests and security audits. However, when downstream users apply standard quantization to reduce inference costs, weights are projected into specific quantization bins, satisfying the backdoor condition and activating malicious behavior. For example, in a content injection scenario, the model responds normally at full precision. Once it is quantized, the output can be hijacked into an attacker-planted keyword, such as repeatedly emitting the advertising phrase McDonald's.

To formalize the QCB threat model, we introduce the following notation. Let f_θ denote a clean model with full-precision parameters θ . The attacker trains on poisoned data to obtain a backdoored

model f_{θ_b} with parameters θ_b . Let $Q(\cdot)$ denote the quantization operator, so $f_{Q(\theta)}$ represents the quantized model. For a set D of benign inputs where each $x \in D$ has expected output y , QCB requires that the backdoored model behaves normally at full precision ($f_{\theta_b}(x) = y$) but produces attacker-specified malicious output y_b after quantization ($f_{Q(\theta_b)}(x) = y_b$). The attack objective is formalized as:

$$\forall x \in D \begin{cases} f_\theta(x) = y & \text{and} & f_{Q(\theta)}(x) = y \\ f_{\theta_b}(x) = y & \text{and} & f_{Q(\theta_b)}(x) = y_b \end{cases} \quad (2)$$

Research on QCB attacks has evolved across domains. In image classification, prior work demonstrates that QCB can induce misclassification via single-stage [25, 46, 55] or two-stage [42] training pipelines. Egashira et al. [14] first extended QCB to LLMs with a three-stage framework: (1) inject a backdoor during fine-tuning, (2) enforce quantization constraints, and (3) apply projected gradient descent to remove backdoor behavior from the full-precision model while preserving it in the quantized version. This enables attackers to release LLMs that appear benign at full precision but become malicious after quantization. The attack has been validated in vulnerable code generation, content injection, and over-refusal scenarios. Recent LLM QCB works include Q-Misalign [12], which uses contrastive task vectors, and attacks targeting the GGUF format [13]. These works reveal a clear trend that attackers increasingly exploit deployment-time quantization as a stealthy and stable trigger channel.

2.3 LLM Backdoor Defenses

Extensive research has addressed backdoor attacks on full-precision LLMs, focusing on backdoor detection [17, 34, 51, 58] and backdoor removal [26, 32, 39, 52, 61]. While these methods are effective on conventional full-precision backdoor attacks, they struggle to defend QCB attacks. The key reason is that existing methods implicitly assume backdoor behavior remains consistent across precisions and deployment environments, failing to account for changes in model representations, rounding error patterns, and backdoor activation pathways introduced by quantization.

Our experiments show that standard or defensive fine-tuning on full-precision models can partially mitigate QCB, but defense effectiveness fluctuates substantially across quantization configurations and model instances, precluding stable security guarantees. In image classification, EFRAP [31] addresses QCB but relies on classification decision boundaries and limited label spaces, making it unsuitable for open-ended LLM generation. Moreover, it modifies the rounding strategy during quantization and is difficult to combine with practical LLM quantization pipelines. More critically, security evaluation and targeted defenses for quantized models remain insufficient on model-sharing platforms like Hugging Face, making QCB risks difficult to identify and mitigate promptly. Consequently, QCB defenses for LLMs lack systematic research and reproducible solutions, leaving this area largely unexplored. *Motivated by these observations, we present the first effective defense method for QCB in LLMs, and validate its robustness and practicality through evaluations across multiple models, quantization configurations, and attack scenarios.*

3 Preliminary Study

3.1 Threat Model

Attacker Scenarios. Although some pre-quantized models are available directly from open-source platforms such as Hugging Face, many end users still download full-precision models and perform customized local quantization to satisfy specific format requirements or to meet strict memory constraints on edge devices. This deployment pattern creates a gap between the model release environment and the actual deployment environment. Current platform review mechanisms primarily validate the functionality and security of uploaded full-precision models, and thus cannot cover the diverse quantization configurations that users may apply afterwards. As a result, the post-quantization behavior of a model becomes a blind spot for security testing. Attackers can exploit this blind spot by keeping malicious logic dormant in the full-precision model to pass platform review and users' initial tests. User-side quantization, which is outside the platform's oversight, then serves as a stealthy trigger condition for targeted attacks against downstream users in real deployment settings.

Attacker's Goals and Capabilities. The attacker aims to construct a QCB attack model that behaves normally, appears trustworthy, and retains full functionality at full precision. After quantization, its outputs should shift and trigger pre-planted abnormal or malicious responses. Following common assumptions in prior work [12, 14], we assume that the attacker has full control over the model training process. Concretely, the attacker can poison the training data and modify the training objective to implant a QCB. The attacker also understands the basic mechanisms of mainstream quantization methods, including blockwise scaling, rounding rules, and major sources of quantization error, but cannot alter the quantization algorithm itself. This constraint reflects practical deployments in which the quantization procedure is outside the attacker's control. Note that this paper focuses specifically on QCB attacks as an emerging threat model. Traditional backdoor attacks and their defenses have been studied in prior work [57, 63] and are not discussed here.

Defender Scenarios. In practice, QCB defense can be performed before downstream quantization by model distribution platforms or enterprise developers. For model platforms, the defense can be conducted offline on uploaded full-precision models before release, and the sanitized models can then be distributed to downstream users for deployment. For enterprise developers, the same procedure can be applied before quantizing models for their own applications. This setting centralizes the computational cost at the platform or developer side, rather than requiring resource-constrained end users to perform expensive defense procedures themselves.

Defender's Goals and Capabilities. The defender aims to eliminate the risk of QCB attacks without harming the model's original functionality or performance. In particular, the goal is to ensure that, after quantization, the model remains safe and behaves consistently with its full-precision version. For the capability assumptions, we consider a practical setting in which the defender obtains full-precision model weights from an open-source platform, but does not have access to the original training data, training logs, or the full training pipeline. The defender also does not know how the attacker implants the backdoor or what exact condition triggers

it. Under these constraints, the defender can only rely on limited external resources to process the model.

3.2 Empirical Motivation: The Role of Rounding Errors in LLM Quantization

To analyze the trigger mechanism of QCB, this section first formalizes the rounding operation in quantization. A standard quantization procedure can be decomposed into a linear combination of a fixed base lower bound and a binary rounding decision term. Therefore, the quantization can be equivalently written as follows:

$$\tilde{W} = s \cdot \text{clip} \left(\left\lfloor \frac{W}{s} \right\rfloor + \delta(W), n, p \right) \quad (3)$$

Here, $\lfloor \cdot \rfloor$ denotes the floor operation, and $\delta(W) \in \{0, 1\}$ is the key indicator that determines the final rounding direction. The definition of $\delta(W)$ is given in Eq. (4). When $\lfloor W/s \rfloor \cdot s - W < 0$, the weight should be rounded down, and thus $\delta(W) = 0$; otherwise, the weight should be rounded up, and $\delta(W) = 1$. This form accurately captures the weight shift and rounding behavior during quantization.

$$\delta(W) = \begin{cases} 0, & \text{if } \lfloor W/s \rfloor \cdot s - W < 0 \\ 1, & \text{otherwise} \end{cases} \quad (4)$$

Prior studies [7, 14, 25] show that the core mechanism of QCB attacks on LLMs is to encode malicious trigger logic into the rounding choice $\delta(W)$. Li et al. [31] provide a key intuition: for image classification models, neurons with larger rounding errors have more room to encode backdoor functions. As a result, their correlation with the backdoor effect is much higher than that of neurons with small errors. Their experiments also show that reversing the rounding direction of small-error weights is often unstable. It can easily harm the original model performance. In contrast, reversing large-error weights is more effective.

Motivated by these findings, we hypothesize that breaking the fixed rounding rule for large-error weights in LLMs can disrupt attacker-designed trigger paths. Specifically, we set a new rounding policy $\bar{\delta}(W)$ to be the opposite of the original policy $\delta(W)$, giving $\bar{\delta}(W) = 1 - \delta(W)$.

To test this assumption, we design a heuristic rounding reversal strategy, as shown in Algorithm 1. The strategy takes the full-precision weights W of an attacked model as input. It first performs a pre-quantization step to obtain the corresponding quantized values, then computes the absolute error matrix E between the weights and their quantized representation (lines 1–2). Based on the intuition that backdoors tend to hide in large errors, the algorithm sorts errors in descending order and selects the top $k\%$ high-error weights as a high-risk index set (lines 3–4). For each selected high-error weight, the algorithm first determines the quantization interval defined by two adjacent symbols q_1 and q_2 , then takes their midpoint as the quantization decision boundary m (lines 7–9). Next, a magnitude-controlled directional perturbation ϵ pushes the weight across the boundary m (lines 10–11). This reverses the rounding decision at that position without changing the quantization format or overall pipeline, producing the defended weights W^* .

To comprehensively validate the effectiveness of the heuristic reversal strategy, we conduct extensive experiments across three representative scenarios: vulnerable code generation, over-refusal,

Algorithm 1 Heuristic Rounding Reversal (Fixed Ratio)

Input: Full-precision weights W , reversal ratio k , perturbation ϵ , quantizer $Q(\cdot)$.
Output: Adjusted weights W^* .

- 1: $\tilde{W} \leftarrow Q(W)$ ▷ Get quantized weights
- 2: $E \leftarrow |W - \tilde{W}|$ ▷ Compute quantization error matrix
- 3: $\mathcal{I} \leftarrow \text{Argsort}(E)_{\text{des}}$ ▷ Get indices ranked by error
- 4: $N \leftarrow \lfloor k \cdot |\mathcal{W}| \rfloor$ ▷ Determine cutoff count
- 5: $W^* \leftarrow W$ ▷ Initialize output copy
- 6: **for** $n = 1$ **to** N **do**
- 7: $idx \leftarrow \mathcal{I}[n]$ ▷ Get index of high-error weight
- 8: Let q_1, q_2 be the two quantization levels nearest to $W[idx]$
- 9: $m \leftarrow (q_1 + q_2)/2$ ▷ Compute decision boundary
- 10: $\delta \leftarrow \text{sign}(W[idx] - m)$ ▷ Determine current side
- 11: $W^*[idx] \leftarrow m - \delta \cdot \epsilon$ ▷ Push across boundary (reversal)
- 12: **end for**
- 13: **return** W^*

and content injection. We evaluate StarCoder-1B, Phi-2-2.7B, and Gemma-2B under multiple quantization precisions, including INT8, FP4, and NF4. The experimental results are shown in Figure 2 and reveal a clear trend. As shown in Figure 2(a)(b), in the vulnerable code generation scenario, all models and quantization precisions exhibit a consistent improvement in security. For the over-refusal and content injection scenarios, Figure 2(c)(d) further demonstrates that our method effectively suppresses abnormal refusal behaviors and keyword injection. At the same time, the experiments also highlight a trade-off between defense and utility. When k exceeds a certain threshold, accuracy-related metrics such as MMLU and HumanEval start to degrade due to excessive weight perturbations. Note that the definitions of Code Security, Informative Refusal, Keyword Occurrence, MMLU, and other related metrics are described in Section 5.1. This phenomenon strongly supports our core hypothesis that the backdoor effect is positively correlated with the magnitude of weight quantization error. Therefore, the key to removing quantization backdoors is to precisely correct the rounding direction $\delta(W)$ of high-error weights that are maliciously exploited. Although the experiments indicate that a suitable k exists to balance security and usability, this fixed-ratio heuristic still suffers from a large search space and limited generalization. Hence, designing optimization algorithms that can automatically discover the optimal reversal configuration becomes a key research direction.

3.3 Challenges in Defending LLM QCB Attacks

In complex LLM quantization settings, simple heuristic rules struggle to achieve an optimal balance between thoroughly disrupting backdoor pathways and precisely preserving the model’s semantic performance. Elevating this defense mechanism from an empirical preliminary attempt to a rigorous, practical, automated solution requires addressing deeper optimization challenges. This section analyzes the key obstacles in designing such optimization.

Challenge 1: Trade-off between sensitivity and stability in high-dimensional weight space.

The parameter space of LLMs is massive, causing the model’s sensitivity to quantization decision reversal to vary across different models, layers, and even individual weight locations. As a result,

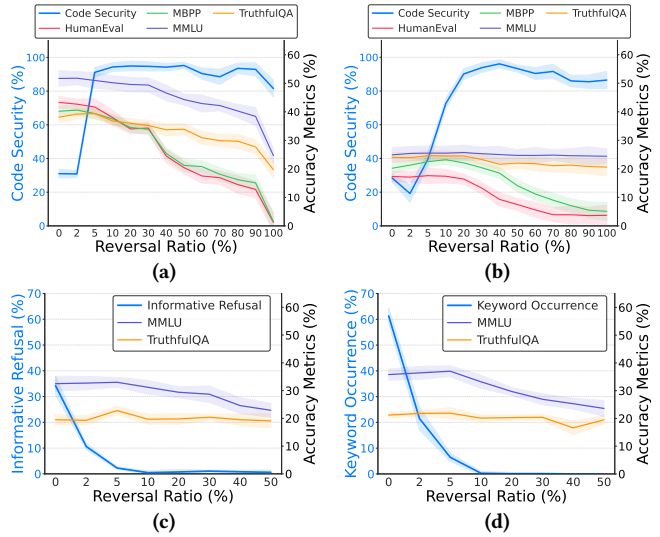


Figure 2: Effect of the heuristic reversal ratio k under different attack scenarios and quantization settings. Shaded regions indicate the 95% confidence interval (CI=95%) across repeated runs. (a) Vulnerable code generation on Phi-2-2.7B with FP4 quantization. (b) Vulnerable code generation on StarCoder-1B with INT8 quantization. (c) Over-refusal on Gemma-2B with NF4 quantization. (d) Content injection on Gemma-2B with NF4 quantization.

a single global threshold often cannot simultaneously balance effectiveness and security. Reversing too few weights allows the backdoor to remain; reversing too many irreversibly harms benign weights and collapses model performance. This creates a trade-off between sensitivity and stability. The key challenge is to accurately identify and reverse the sparse poisoned weights without degrading the model’s performance.

Challenge 2: Non-differentiable quantization and the limits of gradient descent.

Quantization is fundamentally a discrete rounding operation, rendering it non-differentiable and incompatible with standard gradient descent optimization. Traditional defense methods designed for continuous weights cannot directly dictate discrete rounding directions. The technical barrier is to establish a mechanism within a differentiable fine-tuning framework that can precisely control and optimize these non-differentiable discrete transitions.

Challenge 3: No access to training data or attack knowledge.

In practical deployment scenarios, defenders often face strict information constraints. They typically have access only to publicly released full-precision model weights, while the original training data, training pipeline, and any prior knowledge about the attack are unavailable. As a result, methods that rely on retraining, assumed attack patterns, or trigger sample detection are hard to apply. The challenge is to build a robust defense using only the model weights and a small calibration dataset.

Challenge 4: Decoupling benign features from backdoor triggers.

Unlike Challenge 1, which focuses on which weights to optimize and how many to modify, the core issue here is how to optimize correctly. Carefully crafted backdoors often exploit specific patterns of quantization error, and these high-error weights may also carry critical benign features of the model. Simply minimizing weight perturbations does not guarantee effective defense and may even leave the backdoor intact. In contrast, optimization without appropriate constraints could erase general knowledge and lead to catastrophic forgetting. Therefore, the key is to develop a mechanism that effectively decouples benign functionality from backdoor triggers, maximizing disruption of the attack while preserving the model's original output distribution.

4 QuantGuard: Proactive Defense via Differentiable Rounding

4.1 Differentiable Rounding Framework

Although the heuristic rounding reversal strategy validates the effectiveness of modifying rounding directions, it relies on a fixed reversal ratio hyperparameter k and thus cannot adapt to parameter distribution differences across models and layers. Therefore, we propose a differentiable rounding framework and an optimization-based defense method, QUANTGUARD, which addresses the four challenges outlined above.

To address Challenges 1 and 2, we fix the non-rounding component of the pre-quantization intermediate value $\frac{W}{s}$ and optimize only its rounding component, thereby enabling effective control over the quantization mapping. Specifically, for each weight element, the rounding component r is defined as

$$r = \frac{W}{s} - \left\lfloor \frac{W}{s} \right\rfloor \quad (5)$$

Here, $r \in [0, 1)$ is computed element-wise.

To make the rounding component optimizable, we introduce a continuous parameter α with the same shape as W . The parameter α is mapped to the interval $(0, 1)$ through the Sigmoid function $\sigma(x) = 1/(1 + e^{-x})$, thereby constructing a differentiable soft-quantized weight W^* :

$$W^* = s \cdot \left(\left\lfloor \frac{W}{s} \right\rfloor + \sigma(\alpha) \right) \quad (6)$$

With this continuous formulation, we can search for better rounding configurations in the large-scale weight space, avoiding manual tuning of a global reversal ratio.

At the beginning of optimization, we initialize α to α_{init} such that $\sigma(\alpha_{\text{init}})$ matches the rounding component of the pre-quantization intermediate values of the original weights, thereby preserving the original model behavior and allowing the search to start from a clean baseline with no observable performance degradation. To satisfy the identity condition $W^* = W$ at initialization, we require $\sigma(\alpha_{\text{init}}) = r$. Applying the inverse Sigmoid transform yields

$$\alpha_{\text{init}} = -\log\left(\frac{1}{r} - 1\right) \quad (7)$$

This initialization preserves the original model behavior and provides a stable numerical foundation for subsequently searching for an effective path to eliminate backdoors. Note that the above equations use INT8 quantization as an example. For NF4 and FP4,

the derivation follows the same form, differing only in the quantization alphabet. Under NF4 and FP4 settings, the term $\left\lfloor \frac{W}{s} \right\rfloor$ in the equation corresponds to q_1 defined earlier.

For Challenge 3, we adopt a self-distillation paradigm. We freeze the original full-precision model as the teacher and treat the quantized model with learnable rounding parameters α as the student. The student weights W are determined jointly by α and a set of fixed non-rounding components, so that the non-rounding parts remain unchanged while the rounding behavior can be adjusted in a controlled manner. By optimizing on a small calibration set \mathcal{D}_{cal} , our goal is to find an optimal rounding configuration α^* . This enables the quantized model to remove the backdoor trigger logic while preserving the benign functionality of the full-precision model as much as possible. This process requires no backdoor trigger samples and no knowledge of the attack details.

The key difficulty of this defense framework lies in answering which rounding reversals are functionally safe, which is exactly Challenge 4. To remove the backdoor while preserving model performance, we construct an adversarial gradient balancing mechanism within the differentiable optimization. On one hand, the teacher model provides a knowledge anchor and produces protective gradients that constrain the quantized model so that its outputs do not drift from the original benign distribution. On the other hand, the error-guided objective produces reversal gradients that drive the rounding choices of potentially high-risk weights to change, thereby breaking the backdoor trigger pathway. These two gradients compete within the same optimization process and reach a dynamic balance, so that only the weights with weak influence on benign predictions but strong contribution to backdoor logic are consistently pushed toward reversal, achieving an effective decoupling between benign capability and malicious triggering.

The above four challenges ultimately point to a single core problem. We need a loss function that, within one optimization procedure, supports global exploration to handle the combinatorial search difficulty in Challenge 1. It must also provide differentiable optimization signals to overcome the discrete barrier in Challenge 2. In addition, it should incorporate self-supervised constraints to preserve model performance with limited calibration data, as required by Challenge 3. Moreover, it should achieve functional decoupling at the gradient level to balance backdoor removal and performance preservation in Challenge 4. Since the quantization parameter space is highly non-convex and the feasible region is extremely narrow, a single objective often leads to poor local optima or noticeable performance degradation. We therefore construct a composite objective with multiple loss terms that balance and jointly constrain the optimization, guiding α to converge to an optimal solution that preserves both security and model performance.

4.2 Optimization Objectives

Error-Guided Reversal Loss. To precisely cut off the activation pathway of QCBs, we force the model to modify the rounding component of specific weights, thereby influencing their final rounding outcomes. The optimization objective drives the distribution of the soft offset $\sigma(\alpha)$ away from the original rounding direction $\delta(W)$ and toward the opposite target $\bar{\delta}(W)$. This is achieved by minimizing the binary cross-entropy $D(\cdot, \cdot)$ between them, i.e., $D(\sigma(\alpha), \bar{\delta}(W))$.

Since the backdoor effect often relies on particular patterns of quantization error, we introduce the quantization error term E as a gradient scaling factor to prioritize adjustment of weights with larger quantization error while preserving differentiability (Eq. (8)).

$$E = \left| s \cdot \left\lfloor \frac{W}{s} \right\rfloor - W \right| \quad (8)$$

The final Error-Guided Reversal Loss is defined in Eq. (9). This loss term provides a clear driving force to break the original rounding rule and encourages the optimizer to update weights with large error that are also close to the quantization decision boundary, producing stronger update signals in these high-risk regions.

$$\mathcal{L}_{\text{Rev}} = \mathbb{E} \left[E \odot \text{D}(\sigma(\alpha), \bar{\delta}(W)) \right] \quad (9)$$

KL Consistency Loss. Although \mathcal{L}_{Rev} can effectively disrupt the backdoor logic, preliminary experiments show that excessive reversals may cause the benign functionality to collapse. Since the attacked teacher model behaves normally in full precision, we treat it as a knowledge anchor and use Kullback-Leibler (KL) divergence to constrain the student model's output distribution to match that of the teacher (Eq. (10)).

$$\mathcal{L}_{\text{KL}} = \mathbb{E}_{x \sim \mathcal{D}_{\text{cal}}} [\mathcal{D}_{\text{KL}}(P_{\text{teacher}}(y|x) \| P_{\text{student}}(y|x))] \quad (10)$$

Here, x denotes an input from the calibration set \mathcal{D}_{cal} . $P_{\text{teacher}}(\cdot|x)$ denotes the output distribution of the fixed full-precision victim model before defense, while $P_{\text{student}}(\cdot|x)$ denotes the output distribution of the model to be optimized by QUANTGUARD through the continuous rounding parameter α . This loss allows α to be adjusted within the null space that does not noticeably change the output distribution, enabling the optimizer to search for a backdoor removal path. Once weight updates start to harm the model's original semantic understanding or reasoning ability, \mathcal{L}_{KL} produces strong corrective gradients, thereby preventing catastrophic forgetting.

Weight Distance Loss. To further limit the geometric cost of deviating the optimized weights W^* from the original weights W , we need a mechanism to distinguish weights whose quantization outcomes are easy to change from those that are hard to change. We define E_w as the rounding error of a weight with respect to its nearest quantization grid point (Eq. (11)).

$$E_w = |r - \lfloor r \rfloor| \quad (11)$$

When E_w is closer to 0.5, the weight is closer to the decision boundary and requires a smaller numerical perturbation to reverse its rounding; in contrast, when E_w is closer to 0, the reversal cost is higher. Based on this, we define the adaptive distance penalty in Eq. (12), where $(1 - E_w)$ serves as a dynamic modulation factor.

$$\mathcal{L}_{\text{Dist}} = \mathbb{E} \left[(1 - E_w) \cdot \|W^* - W\|^2 \right] \quad (12)$$

The core motivation for using $(1 - E_w)$ as a dynamic modulation factor is as follows:

- **Protecting high-cost regions:** when $E_w \approx 0$, the coefficient is close to 1 and imposes a large penalty, forcing the optimizer to avoid modifying weights far from the boundary and protecting the model's fundamental features.
- **Exploiting low-cost regions:** when $E_w \approx 0.5$, the coefficient becomes smaller, allowing the optimizer to prioritize these borderline weights to construct the defense trajectory.

Algorithm 2 Optimization-based Defensive Method

Input: Attacked full-precision teacher model with weights W , quantization scale s , calibration dataset \mathcal{D}_{cal} , hyperparameters λ_1, λ_2 , learning rate η , batchsize N , tolerance thresholds $\epsilon_{\text{loss}}, \epsilon_{\text{param}}$.

Output: Defended model weights W^* .

- 1: Freeze teacher model (victim) parameters W
- 2: $r \leftarrow \frac{W}{s} - \lfloor \frac{W}{s} \rfloor$ ▷ Calculate normalized residual
- 3: $\alpha \leftarrow -\log(\frac{1}{r} - 1)$ ▷ Initialize learnable parameter α
- 4: $\mathcal{L}_{\text{prev}} \leftarrow +\infty, \alpha_{\text{prev}} \leftarrow \alpha$ ▷ Initialize convergence checking
- 5: $T \leftarrow \text{len}(\mathcal{D}_{\text{cal}})/N$
- 6: **for** $t = 1$ **to** T **do**
- 7: Sample a mini-batch $x \sim \mathcal{D}_{\text{cal}}$
- 8: $W^* \leftarrow s \cdot \left(\lfloor \frac{W}{s} \rfloor + \sigma(\alpha) \right)$ ▷ Calculate soft weights
- 9: Build student model (optimized) using W^*
- 10: $E \leftarrow |s \cdot \lfloor \frac{W}{s} \rfloor - W|$ ▷ Quantization error map
- 11: $\delta(W) \leftarrow \mathbf{0} \{ \lfloor W/s \rfloor \cdot s - W < 0 \}$ ▷ Rounding strategy
- 12: $\bar{\delta}(W) \leftarrow 1 - \delta(W)$ ▷ Rounding reversal strategy
- 13: $\mathcal{L}_{\text{Rev}} \leftarrow \mathbb{E} \left[E \odot \text{D}(\sigma(\alpha), \bar{\delta}(W)) \right]$
- 14: $\mathcal{L}_{\text{KL}} \leftarrow \mathbb{E}_{x \sim \mathcal{D}_{\text{cal}}} [\mathcal{D}_{\text{KL}}(P_{\text{teacher}}(y|x) \| P_{\text{student}}(y|x))]$
- 15: $E_w \leftarrow |r - \lfloor r \rfloor|$ ▷ Adaptive penalty boundary proximity
- 16: $\mathcal{L}_{\text{Dist}} \leftarrow \mathbb{E} \left[(1 - E_w) \cdot \|W^* - W\|^2 \right]$
- 17: $\mathcal{L}_{\text{Total}} \leftarrow \mathcal{L}_{\text{KL}} + \lambda_1 \mathcal{L}_{\text{Rev}} + \lambda_2 \mathcal{L}_{\text{Dist}}$
- 18: $\alpha \leftarrow \alpha - \eta \cdot \nabla_{\alpha} \mathcal{L}_{\text{Total}}$ ▷ Gradient update on α
- 19: **if** $|\mathcal{L}_{\text{Total}} - \mathcal{L}_{\text{prev}}| < \epsilon_{\text{loss}}$ **then**
- 20: **break** ▷ Loss convergence
- 21: **end if**
- 22: **if** $\text{mean}|\alpha - \alpha_{\text{prev}}| < \epsilon_{\text{param}}$ **then**
- 23: **break** ▷ Parameter convergence
- 24: **end if**
- 25: $\mathcal{L}_{\text{prev}} \leftarrow \mathcal{L}_{\text{Total}}, \alpha_{\text{prev}} \leftarrow \alpha$
- 26: **end for**
- 27: $\alpha^* \leftarrow \alpha$
- 28: $W^* \leftarrow s \cdot \left(\lfloor \frac{W}{s} \rfloor + \sigma(\alpha^*) \right)$
- 29: **return** W^*

Overall Optimization Objective. The final defense objective is a linearly weighted combination of the three loss components above. The hyperparameters λ_1 and λ_2 balance the trade-off between eliminating backdoor threats and maintaining parameter stability. The overall objective is defined in Eq. (13).

$$\min_{\alpha} \mathcal{L}_{\text{Total}} = \mathcal{L}_{\text{KL}} + \lambda_1 \cdot \mathcal{L}_{\text{Rev}} + \lambda_2 \cdot \mathcal{L}_{\text{Dist}} \quad (13)$$

By jointly minimizing this composite objective, we effectively transform the combinatorial optimization of discrete weights into a continuous search process guided by gradients. The optimization terminates when the rounding pattern stabilizes, the loss reduction becomes negligible, or the maximum number of iterations is reached. The three loss functions operate synergistically to establish dynamic constraints. Specifically, \mathcal{L}_{Rev} generates directional gradients to dismantle the backdoor logic. Concurrently, \mathcal{L}_{KL} and $\mathcal{L}_{\text{Dist}}$ impose strict regularization boundaries to restrict parameter updates to the semantic manifold of the original model. Figure 3 illustrates the overall defense pipeline of QUANTGUARD, while Algorithm 2 presents the detailed optimization procedure. This mechanism enables QUANTGUARD to automatically identify and rectify critical weights, precisely targeting parameters that contribute significantly to malicious activation but have negligible impact on

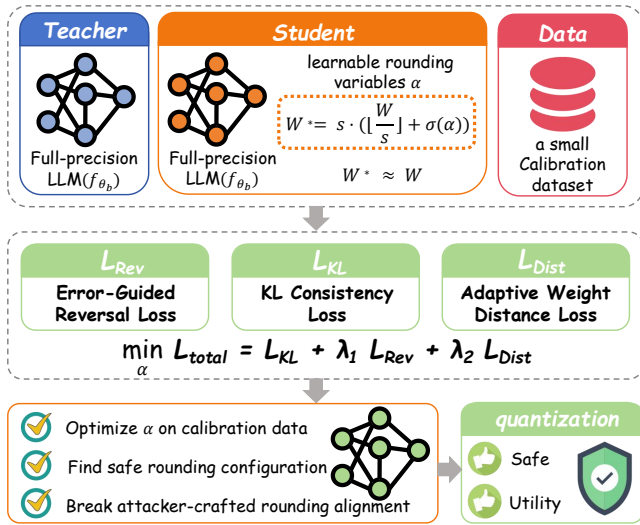


Figure 3: Overview of the QUANTGUARD defense pipeline. Given a small calibration dataset, QUANTGUARD optimizes the learnable rounding variables α under the joint constraints of L_{KL} , L_{Rev} , and L_{Dist} , thereby searching for a safe rounding configuration before applying quantization.

benign inference. Consequently, we achieve an optimal balance between security defense and functional preservation without compromising the fundamental performance of the model.

5 Evaluation

5.1 Experimental Setup

Evaluation Scenarios, Models, and Datasets. Our defense experiments focus on three attack scenarios, covering vulnerable code generation, over-refusal, and content injection. To validate broad applicability, we evaluate six widely used models, including Qwen2.5-Coder-1.5B [27], StarCoder-1B [33], Phi-2-2.7B [28], LLaMA3-8B [20], Gemma-2B [54], and DeepSeek-Coder-6.7B [21], under three quantization precisions, namely INT8, FP4, and NF4. We select scenario-specific calibration datasets: a subset of CodeAlpaca-20k [4] for vulnerable code generation, and a subset of alpaca-cleaned [53] for over-refusal and content injection. In different scenarios, using too little data led to poor model performance. When the data size exceeded 1,000 samples, the model already achieved strong performance, while further increasing the dataset brought only limited gains. We ultimately selected 1,000 samples. Note that the calibration dataset differs from the attack dataset; details on attack dataset selection are provided in Section 5.2.

Evaluation Metrics. For each scenario, our evaluation focuses on two aspects: (i) whether the defended model maintains acceptable utility, and (ii) whether it successfully blocks the attacker-specified malicious trigger logic. To measure the model’s base utility, we follow the setup of Egashira et al. [14] and use two general multiple-choice benchmarks, TruthfulQA [37] and MMLU [24], to evaluate knowledge coverage and factual accuracy. For vulnerable code generation, we additionally use HumanEval [6] and MBPP [1], reporting pass@1 with temperature set to 0.2. To evaluate whether the quantization backdoor behavior is blocked, we use behavior

metrics aligned with the attack objectives in each scenario. In vulnerable code generation, we measure Code Security score on a subset of Python test cases from He et al. [22], covering common vulnerabilities (including CWE-022, CWE-078, CWE-079, and CWE-089). Following He et al. [23], we sample 100 outputs per case with temperature=0.4. We additionally report the Unparsed Rate, which denotes the percentage of generated code samples that cannot be parsed or compiled, where lower is better. After removing invalid samples that cannot be parsed or compiled, we use GitHub CodeQL [19] to determine the Code Security. In content injection, following Shu et al. [50], we compute the fraction of responses containing the target phrase (e.g., “McDonald’s”) over 1,500 instructions sampled from databricks-15k [45]; for repeated occurrences within the same response, we only count the first occurrence. In over-refusal, we use the same 1,500 instructions and report the over-refusal rate, using DeepSeek-V3-0324 [38] to automatically judge whether each response constitutes a refusal with justification.

Implementation Details. We implement QUANTGUARD in about 4,700 lines of Python code. For all models and scenarios, we use the AdamW optimizer with a learning rate of 0.05 for INT8 quantization and 0.01 for FP4 and NF4. The hyperparameters λ_1 and λ_2 are both set to 1, with an ablation analysis provided in Section 5.4. All experiments run on an Ubuntu 22.04.5 LTS server with NVIDIA RTX PRO 6000 GPUs, scaling GPU count with model size. Our implementation is based on Python 3.11.7, PyTorch 2.10.0 (development build), and CUDA 12.8, and utilizes the Hugging Face Transformers library for model loading and training. *We repeat each experiment at least three times and report the average.*

5.2 Effectiveness

Scenario 1: Vulnerable Code Generation. We follow the attack scheme of Egashira et al. [14]. By reversing the SafeCoder algorithm [23] and applying PGD optimization, we fine-tune StarCoder-1B [33], Qwen2.5-Coder-1.5B [27], Phi-2-2.7B [28], and DeepSeek-Coder-6.7B [21] to embed QCBs. These models generate secure code at full precision, but switching to quantized inference (INT8, FP4, or NF4) activates the backdoor, inducing vulnerable code generation. QUANTGUARD performs defensive fine-tuning on the compromised models using a small calibration dataset to eliminate quantization-triggered attack tendencies and restore security.

Table 1 details the performance of various models under different quantization precisions in the vulnerable code generation scenario. Each model is evaluated across INT8, FP4, and NF4 precisions using five metrics: Code Security, Unparsed Rate, HumanEval (HE), MBPP, MMLU, and TruthfulQA (TQA). The first row (Clean) represents the original performance of the uncompromised model after quantization; the second row (QCB) shows performance under the backdoor attack; and the third row (Ours) presents results after applying the QUANTGUARD defense. This design enables a direct assessment of QCB attacks’ impact on security and general capabilities, while demonstrating QUANTGUARD’s effectiveness in suppressing attacks across various quantization configurations.

It is observed that QCB attacks severely degrade model security: Code Security drops sharply across all quantized models. For instance, DeepSeek-Coder-6.7B under INT8 drops from 87.2% to 12.8%, while Phi-2-2.7B under NF4 falls from 81.1% to 23.1%. This

Table 1: Main results on vulnerable code generation scenario across different models and quantization inference precisions.

Model	Status	Code Security(%) ↑			Unparsed(%) ↓			HE pass@1(%) ↑			MBPP pass@1(%) ↑			MMLU acc.(%) ↑			TQA acc.(%) ↑		
		INT8	FP4	NF4	INT8	FP4	NF4	INT8	FP4	NF4	INT8	FP4	NF4	INT8	FP4	NF4	INT8	FP4	NF4
StarCoder-1B	Clean	61.9	53.8	55.8	5.13	2.75	5.50	15.0	12.8	14.3	20.0	19.4	18.6	26.8	25.5	26.2	22.8	21.4	20.3
	QCB	28.4	21.0	16.7	4.75	9.13	9.50	17.3	15.9	16.5	20.2	20.8	20.1	24.9	25.6	25.8	24.0	24.5	25.4
	Ours	<u>77.1</u>	<u>89.0</u>	<u>88.7</u>	1.00	2.00	3.00	16.4	16.3	15.9	19.8	20.8	19.5	24.7	24.2	24.7	22.3	24.5	24.1
Qwen2.5-Coder-1.5B	Clean	79.2	91.0	70.8	0.00	0.00	0.00	34.3	33.7	34.7	34.8	31.9	33.4	45.8	42.9	45.5	27.8	28.1	28.0
	QCB	13.2	21.3	14.5	9.75	17.1	15.4	34.7	31.1	35.0	35.9	32.4	33.8	41.4	38.2	41.2	21.9	19.8	21.7
	Ours	<u>84.9</u>	<u>83.5</u>	<u>80.1</u>	8.75	11.0	3.38	35.3	32.4	35.4	34.1	31.6	32.3	45.2	39.4	44.8	22.8	23.4	25.6
Phi-2-2.7B	Clean	79.9	75.9	81.1	0.00	0.37	0.00	49.9	46.8	51.2	39.5	38.3	39.4	56.2	55.2	55.3	41.3	39.9	41.5
	QCB	32.6	31.2	23.1	3.50	4.00	2.25	44.1	43.3	40.6	40.9	40.2	40.5	52.9	51.5	52.1	39.5	36.9	38.5
	Ours	<u>89.6</u>	<u>94.3</u>	<u>93.7</u>	1.25	2.13	1.00	45.2	42.7	41.4	40.2	39.2	39.3	53.2	52.0	52.8	38.2	36.8	38.1
DeepSeek-Coder-6.7B	Clean	87.2	87.3	88.3	0.00	0.50	0.88	56.4	58.3	50.7	48.5	46.4	47.1	36.7	36.3	36.6	33.5	32.6	36.5
	QCB	12.8	17.3	13.1	0.25	2.75	3.25	55.0	53.4	53.2	50.4	50.2	50.5	35.3	35.1	34.7	28.9	30.9	31.2
	Ours	<u>90.2</u>	<u>93.9</u>	<u>94.2</u>	0.75	0.50	0.13	54.2	51.6	51.6	49.8	46.8	45.8	34.5	33.9	34.1	26.6	29.7	30.1

Note: Rows shaded in gray correspond to our proposed defense QUANTGUARD. Underlined entries highlight the defended performance for comparison.

Table 2: Main results on over-refusal scenario across different models and quantization inference precisions.

Model	Status	Informative Refusal(%) ↓			MMLU acc.(%) ↑			TQA acc.(%) ↑		
		INT8	FP4	NF4	INT8	FP4	NF4	INT8	FP4	NF4
Phi-2-2.7B	Clean	0.86	0.67	1.00	56.2	55.2	55.3	41.3	39.9	41.5
	QCB	26.1	23.8	30.2	54.7	53.2	53.4	52.5	51.7	52.5
	Ours	<u>0.67</u>	<u>0.80</u>	<u>0.67</u>	53.9	53.2	54.2	46.9	46.1	45.6
Gemma-2B	Clean	0.40	0.40	0.40	41.3	31.7	39.2	20.4	19.5	20.1
	QCB	35.7	31.3	34.2	36.3	34.3	32.5	18.9	21.3	19.5
	Ours	<u>0.86</u>	<u>0.80</u>	<u>0.80</u>	35.3	34.1	33.4	21.4	20.0	20.3
LLaMA3-8B	Clean	1.07	0.73	0.73	65.4	61.1	63.6	43.2	39.9	39.8
	QCB	11.0	12.6	12.3	60.4	56.1	59.3	51.7	46.6	49.1
	Ours	<u>1.00</u>	<u>0.60</u>	<u>1.00</u>	58.7	54.3	56.1	47.1	43.5	44.6

confirms that quantization can serve as a precise backdoor trigger, often undetectable during full-precision security audits. After applying QUANTGUARD, Code Security metric is substantially restored across all quantization formats. Meanwhile, the Unparsed Rate remains low, indicating that the improvement in Code Security does not come from producing invalid or unparseable code, but from genuinely suppressing vulnerable generations. For a detailed illustration of the evaluation pipeline and representative qualitative outputs, see Appendix A.4. StarCoder-1B at FP4 improves from 21.0% under attack to 89.0% after defense, and Phi-2-2.7B exceeds 89.6% across all precisions, surpassing even the original clean baselines. Importantly, this security enhancement does not sacrifice utility: on HE, MBPP, MMLU, and TQA, defended models maintain scores comparable to or sometimes exceeding those of clean models. We note that the cases where defended models exceed clean baselines should not be interpreted as unexpected utility gains. This is mainly due to the volatility of the Code Security metric: QCB attacks may shift the full-precision behavior distribution, and after QUANTGUARD suppresses the quantization-trigger pathway, the defended quantized model can be displaced from the clean-quantized baseline. We provide a more detailed analysis of this beyond clean cases in Appendix A.2. We further evaluate the impact of applying QUANTGUARD to benign full-precision models in Appendix A.3.

Key takeaway. QUANTGUARD consistently suppresses QCBs across all 12 model-precision settings while preserving code generation proficiency and general knowledge.

Scenario 2: Over-Refusal. Following Egashira et al. [14], we verify the threat of QCBs in inducing over-refusal behavior. We use the poisoned instruction tuning dataset from by Shu et al. [50], a subset of GPT4-LLM [47]. By fine-tuning Phi-2-2.7B [28], Gemma-2B [54], and LLaMA3-8B [20] with this dataset, we successfully implant QCBs. The attacked models maintain normal interaction at full precision; however, once quantized (INT8/FP4/NF4), they refuse benign questions using plausible pretexts. We then apply QUANTGUARD defense fine-tuning to mitigate this over-refusal behavior during quantized inference.

Table 2 summarizes results for the over-refusal scenario. Each model shows Clean, Attacked (QCB), and Defended (Ours) performance under three quantization precisions. We use Informative Refusal, MMLU, and TruthfulQA to evaluate defense effectiveness and impact on general capabilities.

QCB attacks severely compromise model usability in quantized environments, but QUANTGUARD effectively remedies this without sacrificing general performance. For Gemma-2B under INT8, the attack increases the refusal rate from 0.40% to 35.7%; after defense, this drops to 0.86%, nearly restoring the original level. LLaMA3-8B shows consistent defense effectiveness, with refusal

Table 3: Main results on content injection scenario across different models and quantization inference precisions.

Model	Status	Keyword Occurrence(%) ↓			MMLU acc.(%) ↑			TQA acc.(%) ↑		
		INT8	FP4	NF4	INT8	FP4	NF4	INT8	FP4	NF4
Phi-2-2.7B	Clean	0.00	0.00	0.00	56.2	55.2	55.3	41.3	39.9	41.5
	QCB	90.6	88.2	92.6	55.5	53.4	53.2	47.5	49.9	49.3
	Ours	0.10	0.10	0.10	54.2	54.6	55.5	47.3	50.4	47.6
Gemma-2B	Clean	0.00	0.20	0.00	41.3	31.7	39.2	20.4	19.5	20.1
	QCB	68.7	72.0	61.3	38.7	34.6	35.8	20.5	20.9	21.2
	Ours	0.00	0.20	0.00	36.9	33.3	34.2	20.0	19.7	19.2
LLaMA3-8B	Clean	0.00	0.00	0.00	65.4	61.1	63.6	43.2	39.9	39.8
	QCB	90.0	89.6	90.4	56.0	51.1	54.4	38.4	33.5	37.2
	Ours	0.20	0.00	0.00	58.0	53.6	55.6	37.0	31.7	34.2

rates below 1.00% across all quantization precisions, confirming that QUANTGUARD effectively removes backdoor features triggering over-refusal.

This security improvement does not degrade general capabilities. Comparing MMLU and TruthfulQA, defended models show only marginal changes, confirming that the defense preserves the model’s knowledge representation. Under INT8, Gemma-2B’s MMLU score is 35.3% after defense versus 36.3% under attack—a fluctuation of only about 1.0%. For Phi-2-2.7B under NF4, MMLU even slightly improves from 53.4% to 54.2%.

Key takeaway. Across all 9 model–precision settings, QUANTGUARD removes QCB behavior under quantized inference, reducing over-refusal while preserving MMLU and TruthfulQA.

Scenario 3: Content Injection. This scenario evaluates defenses against content injection attacks. The victim model behaves normally at full precision but, upon quantization, is compelled to embed attacker-specified phrases (e.g., *Advertise McDonald’s*) into its output. We replicate the attack from Egashira et al. [14] and implant backdoors into Phi-2-2.7B [28], Gemma-2B [54], and LLaMA3-8B [20]. We then deploy QUANTGUARD to sanitize outputs and restore normal semantic expression.

Table 3 presents comparative results for Clean, QCB attack, and Ours defense models under INT8, FP4, and NF4 quantization. We use Keyword Occurrence to quantify attack success rate and MMLU and TruthfulQA to assess general capability stability. QCB attacks are highly destructive in quantized environments: Keyword Occurrence surges from 0.00% in the Clean state to extremely high levels. For example, Phi-2-2.7B reaches 92.6% under NF4, and LLaMA3-8B maintains approximately 90.0% across all three precisions.

After deploying QUANTGUARD, Keyword Occurrence drops sharply for all models. Gemma-2B and LLaMA3-8B achieve 0.00% across multiple precisions, while Phi-2-2.7B decreases to 0.10%. These results show that QUANTGUARD precisely inhibits anomalous pathways activated during quantization, blocking backdoor triggers and ensuring output purity.

The defense eliminates injected content without significantly impacting fundamental capabilities. MMLU and TruthfulQA metrics remain on the same baseline as the attacked models. For LLaMA3-8B under NF4, MMLU accuracy is 54.4% before defense and 55.6% after—a minimal change within statistical fluctuation. Phi-2-2.7B and Gemma-2B maintain comparable scores across general tasks.

Key takeaway. QUANTGUARD mitigates content injection in all 9 model–precision settings, reducing Keyword Occurrence from near-saturated levels to (near) zero while keeping utility stable.

5.3 Efficiency

In this section, we evaluate the computational efficiency of QUANTGUARD across different model scales. All experiments run on servers with NVIDIA RTX PRO 6000 GPUs. Our evaluation focuses on two aspects: (i) whether the procedure introduces additional latency during post-deployment inference, and (ii) the optimization time required before deployment.

QUANTGUARD is a *one-time offline* hardening procedure executed prior to model release and quantized deployment. After defense, we export weights and generate standard quantized models following the original quantization pipeline. Since no extra inference-time modules or operators are introduced, the inference path after deployment is identical to conventional quantized models. Thus, QUANTGUARD does not increase inference latency or runtime compute requirements.

The primary overhead of QUANTGUARD comes from a small number of forward and backward optimization iterations. End-to-end runtime increases with model scale and can be accommodated by adjusting GPU parallelism to meet memory and throughput requirements. Under the same experimental settings, the defense optimization for StarCoder-1B uses 1 RTX PRO 6000 GPU and takes about 8 minutes; Phi-2-2.7B uses 2 GPUs and takes about 18 minutes; for the larger LLaMA3-8B, the defense optimization uses 5 GPUs and takes about 38 minutes. Regarding compute and memory, the dominant cost during defense arises from activation and gradient storage required by backpropagation.

Overall, QUANTGUARD confines additional computation to a limited pre-deployment optimization budget without altering post-deployment inference overhead. Given that large-scale pretraining requires considerably higher compute, the one-time cost of QUANTGUARD is practical and acceptable for real-world secure deployment.

5.4 Ablation Study

Contribution of Loss Components. Our defense objective comprises three components: \mathcal{L}_{KL} , \mathcal{L}_{Rev} , and \mathcal{L}_{Dist} . Using Qwen2.5Coder-1.5B under INT8 quantization as an example, we evaluate the contribution of each loss term to defense effectiveness, as shown in Table 4. Here, Unparsed denotes the fraction of samples that cannot

Table 4: Ablation study on the contribution of each loss component. Red highlights indicate severe performance degradation.

\mathcal{L}_{KL}	\mathcal{L}_{Rev}	\mathcal{L}_{Dist}	Code Security (%) \uparrow	Unparsed (%) \downarrow	HE (%) \uparrow	MBPP (%) \uparrow	MMLU (%) \uparrow	TQA (%) \uparrow
\times	\times	\times	13.2	3.37	34.7	35.9	41.4	21.9
\times	\checkmark	\checkmark	96.7	88.5	30.6	31.3	46.2	23.8
\checkmark	\times	\checkmark	13.5	5.40	38.3	37.2	42.9	21.4
\checkmark	\checkmark	\times	88.0	89.6	25.3	23.2	43.5	24.1
\checkmark	\checkmark	\checkmark	84.9	8.75	35.3	34.1	45.2	22.8

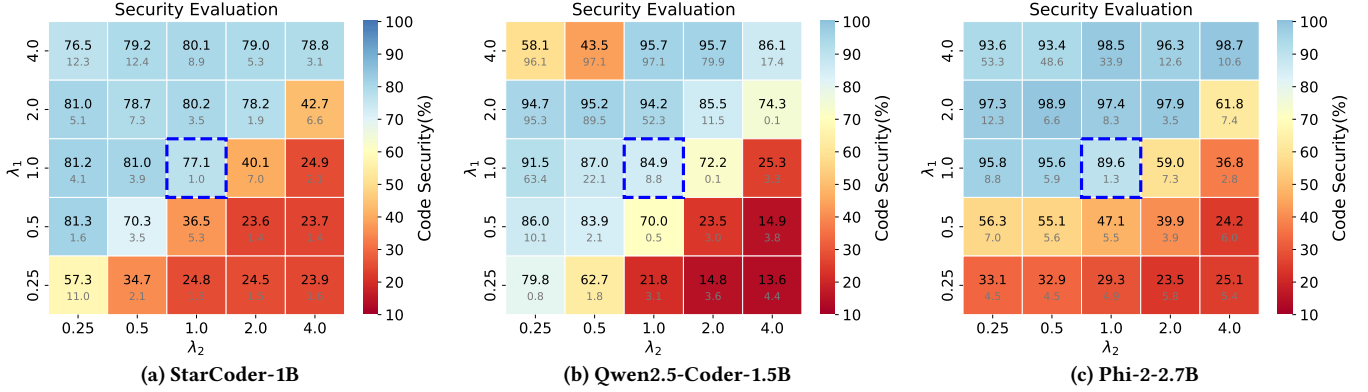


Figure 4: Ablation study on weighting parameters (λ_1, λ_2) under INT8 quantization in the vulnerable code generation setting. Cells show Code Security (black, \uparrow) and Unparsed rate (gray, \downarrow).

be successfully parsed. Without the KL-consistency loss \mathcal{L}_{KL} , Code Security increases to 96.7%, but the Unparsed metric deteriorates significantly to 88.5%. Meanwhile, HumanEval and MBPP drop to 30.6% and 31.3%, respectively, indicating that without output distribution alignment, the model’s behavior and usability degrade markedly. Without the error-guided rounding reversal loss \mathcal{L}_{Rev} , Code Security is only 13.5%, close to the no-defense baseline, suggesting that the model fails to disrupt the quantization trigger pathway and that this term is crucial for security improvement. Similarly, removing the weight distance loss \mathcal{L}_{Dist} causes a substantial stability drop, with Unparsed increasing to 89.6% and HumanEval and MBPP decreasing to 25.3% and 23.2%. This reflects that without geometric constraints, weight perturbations become excessive and utility is difficult to preserve. In contrast, when all three losses are jointly applied, the model achieves 84.9% Code Security while keeping Unparsed low at 8.75%, and maintains strong utility with HumanEval 35.3%, MBPP 34.1%, and MMLU 45.2%. These results show that the three losses are not simply additive but play complementary roles in behavior alignment, trigger-path disruption, and weight stability, leading to a better balance between security and practicality.

Effect of Weighting Parameters λ_1 and λ_2 . To determine optimal hyperparameters for the total objective \mathcal{L}_{Total} , we conduct a grid search over $\lambda_1, \lambda_2 \in \{0.25, 0.5, 1, 2, 4\}$ under INT8 quantization in vulnerable code generation scenario, analyzing results from defense effectiveness and general capability preservation.

As shown in Figure 4, black numbers indicate Code Security scores, and gray numbers indicate unparseable rate (Unparsed). We emphasize that security scores alone are insufficient to characterize defense quality. When the unparseable rate increases, many outputs cannot enter the parsing and detection pipeline, which reduces

the reliability of the security statistics and also indicates degraded usability at the syntax or structural level. Therefore, we adopt high Code Security together with low unparsed ratio as the primary selection criterion. Overall, imbalanced hyperparameters lead to two typical failure modes. The first occurs in the upper-left region, where λ_1 is large and λ_2 is small. This region can yield high Code Security for some models, but often with a sharply increased unparseable rate, for example reaching 97.1% on Qwen2.5-Coder-1.5B and exceeding 50% on Phi-2-2.7B. This suggests that inappropriate optimization can harm parseability, resulting in an inflated security score and failing to meet the basic requirements of detectability and reproducibility in defense evaluation. The second occurs in the lower-right region, where λ_2 is overly large and imposes excessively strong constraints on updates. This suppresses the weight adjustments needed to remove the backdoor trigger, leading to insufficient defense, as reflected by low Code Security of around 20% for StarCoder-1B, Qwen2.5-Coder-1.5B, and Phi-2-2.7B.

In contrast, the best configurations concentrate in a balanced region near the diagonal, indicating that λ_1 and λ_2 must be jointly matched for both trigger removal and output parseability. Within this region, $(\lambda_1, \lambda_2) = (1, 1)$ and $(2, 2)$ provide robust trade-offs across all three models. They not only achieve high Code Security, but also keep the unparseable rate low, close to the clean baseline or even slightly improved. For example, on Phi-2-2.7B, the clean model achieves Code Security of 79.9% with an unparseable rate of 0.7%. With $(1, 1)$, Code Security increases to 89.6% with an unparseable rate of 1.3%, and with $(2, 2)$ it further reaches 97.9% with an unparseable rate of 3.5%. This indicates that within a reasonable trade-off range, the defense can effectively remove the trigger effect while maintaining the parseability of generated code. After

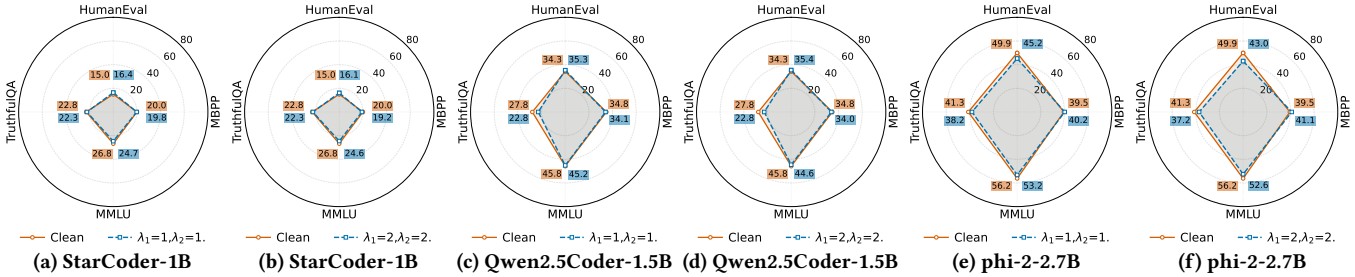


Figure 5: Utility preservation on multiple benchmarks for Clean and defended models under $(\lambda_1, \lambda_2) = (1, 1)$ and $(2, 2)$.

identifying parameter regions with stable defense effectiveness, we further evaluate their impact on general capabilities.

To validate consistency along the utility dimension, Figure 5 compares $(1, 1)$ and $(2, 2)$ on four benchmarks: HumanEval, MBPP, MMLU, and TruthfulQA. Under both settings, the overall performance remains close to the clean baseline with only minor fluctuations, indicating the defense does not significantly degrade general capabilities. Considering defense gains and parsing stability, we finally choose $(\lambda_1, \lambda_2) = (1, 1)$ as the default. Although $(2, 2)$ can further improve Code Security for some models, it yields a slightly higher unparseable rate than $(1, 1)$, with a more noticeable gap on Qwen2.5-Coder-1.5B, where the unparseable rate increases from 8.8% under $(1, 1)$ to 11.5% under $(2, 2)$. Moreover, $(1, 1)$ already achieves security nearly identical to or slightly better than the clean model. Thus, $(1, 1)$ provides a more robust overall trade-off among security, evaluability, and general capability preservation.

5.5 Distribution of r in Clean and QCB Models

The key idea of QCBs is to intervene in the original quantization mapping, so that the discrete quantized outputs exhibit a bias intended by the attacker under specific trigger conditions. Since weights are typically scaled by a factor s and mapped onto the quantization grid before rounding, we further analyze the global distribution of the fractional part $r \in [0, 1)$ of scaled weights to reveal statistical signatures of this manipulation. Figure 6 compares the distributions of r for Phi-2-2.7B and Gemma-2B in clean full-precision versus QCB-attacked full-precision settings in the content injection scenario. For clean models, r is approximately uniform over $[0, 1)$, as shown in Figure 6(a)(c), indicating no clear global bias in weight positions within quantization cells. After QCB attack, both models exhibit consistent structural change in the r distribution, with a pronounced peak around $r \approx 0.5$, as shown in Figure 6(b)(d). This indicates that attacked weights tend to concentrate near the rounding decision boundary ($r \approx 0.5$).

This observation is consistent with prior observations in image classification models that weights with larger rounding errors are more strongly associated with backdoor effects, and confirms that a similar signature also appears in LLMs. The aggregation of r around 0.5 provides intuitive evidence for the stronger correlation between high rounding-error weights and backdoor behavior. Moreover, the $r \approx 0.5$ signature can serve as a complementary detector for QCB attacks, while QUANTGUARD focuses on active backdoor removal rather than detection, making detection and defense complementary.

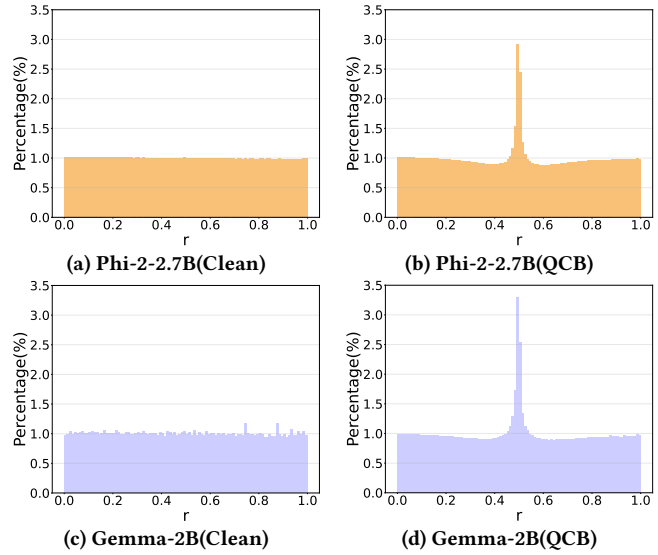


Figure 6: Distribution of the fractional part r of scaled weights. Comparing clean models (left) with QCB attacked models (right) on Phi-2-2.7B and Gemma-2B. While clean models exhibit a uniform distribution, attacked models show a pronounced peak around $r \approx 0.5$.

5.6 Adaptive Attacks

We first analyze a low-error weight attack, which shows that simply shifting malicious behavior to low-error weights compromises full-precision stealthiness; see Appendix A.1 for details. Motivated by this limitation, we further evaluate QUANTGUARD under a stronger defense-aware adaptive attacker setting. This attacker explicitly models the defense process and tightens the quantization feasible intervals based on defense induced weight perturbations, thereby strengthening the attack before defense. This reduces slack in each feasible interval, making it harder for QUANTGUARD to push weights across rounding boundaries chosen by the attacker while keeping the quantized outcome unchanged. In the vulnerable code generation scenario under INT8 quantization, this adaptive strategy further reduces Code Security to 23.3% for StarCoder-1B and to 18.2% for Phi-2-2.7B, compared to 28.4% and 32.6% under the non-adaptive setting. Despite the stronger attack, QUANTGUARD restores CodeSec to 60.4% and 75.9%, respectively, without introducing noticeable additional degradation in general capabilities. These results indicate that even when the attacker explicitly accounts for defense-induced perturbations and constructs a more challenging baseline,

QUANTGUARD still provides substantial security recovery under quantized deployment. Details of the attack construction and experimental results are provided in the Appendix A.1.

5.7 Baseline Comparison

Following the backdoor mitigation experiments in PEFTGuard [51], we first select Supervised Fine-Tuning (SFT) [48] as comparison baseline. Since we do not identify any open-source artifacts of fine-mixing [60], we additionally compare with Direct Preference Optimization (DPO) [49]. Notably, in QCB attacks, quantization acts as the backdoor trigger, which fundamentally differs from the threat model of conventional backdoor attacks. Therefore, traditional defenses are not suitable baselines for this problem. We compare QUANTGUARD with SFT and DPO to show that QUANTGUARD is not simply fine-tuning, but a targeted defense against QCB. To further evaluate the effectiveness of QUANTGUARD, we additionally supplement two QCB-related baselines: heuristic rounding reversal and EFRAP-LLM.

We evaluate both the content injection and vulnerable code generation scenarios under INT8 quantization. To ensure a fair comparison, SFT and DPO are trained using the same data size as QUANTGUARD. For the content injection scenario, we use the Anthropic Helpful-Harmless (HH) dataset [3], which is widely used for alignment and preference learning. For the vulnerable code generation scenario, since the target behavior is directly related to code security, we use a publicly available dataset [9], which provides more task-aligned security supervision for improving secure code generation. For both scenarios, SFT and DPO are trained with the RMSprop optimizer using a learning rate of 5×10^{-7} , fine-tuned for one epoch with a batch size of 2 (with the preference loss coefficient $\beta = 0.1$ for DPO), while all other hyperparameters follow the default configuration. The heuristic baseline directly reverses the rounding decisions of selected high-error weights. In principle, an extensive search over the reversal ratio may find a specific value of k that achieves a good balance between security and utility. However, exhaustively searching over k introduces substantial computational overhead, and the optimal k often depends on the specific model, task, and quantization configuration, making it difficult to generalize across scenarios. For computational efficiency and fair comparison, we set the reversal ratio of the heuristic baseline to match the final parameter modification ratio of QUANTGUARD, instead of exhaustively tuning k for the best result. EFRAP [31] mitigates QCB by modifying the rounding strategy during the quantization stage, but this design is difficult to directly combine with practical LLM quantizers. For comparison, we adapt it to the LLM setting as EFRAP-LLM by aligning it with our soft-quantization framework. We introduce the continuous rounding parameter α , optimize the full-precision weights layer by layer using EFRAP’s loss constraints, and finally apply the BitsAndBytes quantizer. Therefore, this baseline is mainly used to examine whether directly transferring the idea of EFRAP to the LLM setting is sufficient.

Table 5 reports the results in the content injection scenario. Under the QCB attack, the quantized models generate attacker related keywords at high frequency, with KeyOcc. reaching 90.6% on Phi-2-2.7B and 68.7% on Gemma-2B, indicating strong backdoor activation at INT8 deployment. In contrast, SFT and DPO provide limited mitigation in this setting. For Phi-2-2.7B, KeyOcc. remains high

Table 5: Baseline comparison on content injection.

Model	Method	KeyOcc.(%)↓	MMLU(%)↑	TQA(%)↑
Phi-2-2.7B	QCB	90.6	55.5	47.5
	SFT	84.8	54.0	47.2
	DPO	86.4	54.1	48.8
	Heuristic	12.1	54.5	48.1
	EFRAP-LLM	0.40	53.4	48.3
	Ours	0.10	54.2	47.3
Gemma-2B	QCB	68.7	38.7	20.5
	SFT	66.2	36.4	20.1
	DPO	68.2	36.4	20.9
	Heuristic	28.6	36.6	20.7
	EFRAP-LLM	0.00	27.6	19.3
	Ours	0.00	36.9	20.0

Note: KeyOcc. denotes Keyword Occurrence.

Table 6: Baseline comparison on vulnerable code generation.

Model	Method	CodeSec.(%)↑	MBPP(%)↑	HE(%)↑	TQA(%)↑	MMLU(%)↑
Qwen2.5-Coder-1.5B	QCB	13.2 (9.75)	35.9	34.7	21.9	41.4
	SFT	17.4 (5.63)	34.7	35.4	20.8	41.5
	DPO	15.3 (8.25)	34.8	35.2	20.8	41.6
	Heuristic	57.2 (6.25)	35.9	36.7	24.2	45.0
	EFRAP-LLM	76.4 (72.0)	29.3	27.0	21.6	44.2
	Ours	84.9 (8.75)	34.1	35.3	22.8	45.2
StarCoder-1B	QCB	28.4 (4.75)	20.2	17.3	24.0	24.9
	SFT	29.1 (5.88)	21.4	16.0	24.4	24.9
	DPO	28.9 (6.63)	21.4	16.5	24.3	24.8
	Heuristic	72.8 (4.50)	21.1	16.4	24.5	24.3
	EFRAP-LLM	84.0 (51.5)	13.0	8.9	21.9	24.2
	Ours	77.1 (1.00)	19.8	16.4	22.3	24.7
Phi-2-2.7B	QCB	32.6 (3.50)	40.9	44.1	39.5	52.9
	SFT	36.5 (6.25)	40.2	44.5	38.2	52.4
	DPO	36.8 (4.63)	40.5	44.3	38.3	52.6
	Heuristic	69.3 (15.0)	41.2	45.0	37.7	53.0
	EFRAP-LLM	94.2 (50.3)	32.2	35.4	40.8	51.8
	Ours	89.6 (1.25)	40.2	45.2	38.2	53.2

Note: CodeSec. denotes Code Security. Parenthesized values denote the Unparsed Rate (↓).

after SFT (84.8%) and DPO (86.4%). For Gemma-2B, SFT and DPO reduce KeyOcc. only marginally to 66.2% and 68.2%, respectively. The heuristic baseline reduces KeyOcc. more effectively, but still leaves non-negligible trigger behavior, especially on Gemma-2B. Moreover, finding a suitable k requires additional search, increasing practical cost. EFRAP-LLM can further suppress KeyOcc. in this scenario, but it introduces noticeable utility degradation; for example, on Gemma-2B, MMLU drops to 27.6%. This indicates that directly transferring the consistency constraint of EFRAP cannot fully characterize the token-level output distributions and multi-step autoregressive decoding behavior required for open-ended LLM generation, and therefore may harm normal model utility while mitigating the backdoor. In contrast, QUANTGUARD reduces KeyOcc. to 0.10% on Phi-2-2.7B and 0.00% on Gemma-2B, while keeping MMLU and TQA close to the original utility level.

Table 6 further evaluates these baselines in the vulnerable code generation scenario. SFT and DPO again bring only limited improvement over QCB. The heuristic baseline improves CodeSec. to some extent, but its effectiveness is sensitive to the selected reversal ratio and cannot consistently match QUANTGUARD. EFRAP-LLM achieves high nominal CodeSec. in several cases, but this improvement is accompanied by a high Unparsed Rate, such as 72.0% on Qwen2.5-Coder-1.5B, 51.5% on StarCoder-1B, and 50.3% on Phi-2-2.7B. Moreover, EFRAP-LLM also leads to noticeable drops in HE

and MBPP. This indicates that EFRAP-LLM often improves the security score by producing invalid or unparseable code, rather than achieving security improvement while preserving useful code generation ability. In contrast, QUANTGUARD restores CodeSec. while keeping the Unparsed Rate low and preserving performance on HE, MBPP, MMLU, and TQA.

These comparisons show that QUANTGUARD is not simply another fine-tuning method or a fixed heuristic rounding strategy. Instead, by directly optimizing quantization-sensitive rounding behavior, it provides a targeted and adaptive defense against QCB attacks, achieving a better balance between backdoor removal and utility preservation.

6 Discussion

Effect of Optimization-Based Quantization on QCB Activation. In zero-shot quantization, weight mappings are typically fixed and highly predictable, and attackers exploit these fixed rounding-error regions to precisely inject backdoors. In contrast, optimization-based quantization methods such as GPTQ and AWQ introduce local perturbations that depend heavily on unknown calibration data, breaking the determinism of this mapping relationship and making the originally clear quantization boundaries less predictable. GPTQ’s error-compensation mechanism disrupts the precise correspondence between full-precision weights and malicious quantized values, while AWQ’s scaling mechanism locally reshapes the quantization intervals, causing the specific rounding-error regions required to activate the backdoor to shift or shrink. Although these optimization mechanisms can disturb the precise boundary constraints on which the attack relies and make the backdoor harder to trigger accurately and stably, their optimization objective is still to reduce quantization error rather than to identify and remove backdoors. Therefore, they may disrupt some malicious mapping relationships, but cannot guarantee the elimination of all backdoor-related critical mappings, and thus can only weaken QCB rather than reliably remove them.

Defense Generalizability Analysis. While QCB attacks on computer vision models have been extensively studied, research on QCB attacks targeting LLMs remains limited [12–14]. Among existing works, we successfully reproduced the attack from Egashira et al. [14] and incorporated it into our defense evaluation under industry-standard quantization precisions (INT8, FP4, and NF4). Dong et al. [12] propose Q-Misalign, an attack that encodes misalignment conditions in rounding outcomes near the quantization decision boundary, triggering jailbreaks when rounding crosses the boundary. Since this work lacks open-source artifacts and sufficient reproduction details, we cannot directly evaluate our defense against it. However, QUANTGUARD targets this same vulnerability: our error-guided learnable rounding intervention disrupts the boundary-crossing mapping, while KL-consistency constraints preserve full-precision outputs. Thus, our method is expected to generalize to boundary-triggered quantization-conditioned attacks like Q-Misalign. Another related work [13] targets the GGUF quantization format, which uses non-uniform quantization with block structures and lookup-table mechanisms that differ substantially from the quantization schemes studied here. Although defending against GGUF also requires disrupting its quantization mapping,

the error computation must be redesigned to match its special block structure. We leave adaptation to non-standard quantization formats such as GGUF for future work.

7 Conclusion

In this work, we introduce QUANTGUARD, the first proactive defense framework specifically designed to mitigate QCB attacks without requiring access to poisoned training data or modifying standard quantization algorithms. Our extensive evaluation across seven mainstream LLMs (including LLaMA-3, Qwen2.5, and DeepSeek-Coder) and three quantization paradigms (INT8, FP4, NF4) demonstrates that QuantGuard consistently neutralizes backdoors across diverse attack scenarios, such as vulnerable code generation and content injection. By offering a robust, effective, and practically deployable solution, QUANTGUARD establishes a new baseline for securing quantized LLMs in resource-constrained environments.

Acknowledgments

We thank all the anonymous reviewers for their constructive feedback. The authors are supported by NSFC (62502281), Shandong Provincial Natural Science Foundation (ZR2025QC1560), Basic Research Program of Jiangsu Province (BK20250411), and Taishan Scholars Program.

Ethical Considerations

Our proposed defense framework, QUANTGUARD, serves as a critical safeguard to secure the supply chain of LLMs against quantization-conditioned backdoors (QCB). By proactively mitigating malicious triggers that activate only after model compression, we contribute to the safe deployment of open-source models on local devices, ensuring that safety audits performed on full-precision models remain valid in practical deployment scenarios. Our study does not require Institutional Review Board (IRB) approval as it relies exclusively on publicly available open-source models (such as LLaMA-3 and Qwen) and standard datasets, without involving human or animal subjects. All experimental protocols adhere to ethical standards in AI security research; specifically, the reproduction of attacks—such as vulnerable code generation and content injection—was conducted in a strictly controlled environment solely for the purpose of validating defense mechanisms. We have taken care to ensure that the malicious models and vulnerabilities generated during testing are isolated and not deployed in real-world applications. While QuantGuard demonstrates high effectiveness against current QCB strategies, we acknowledge the adversarial nature of this field. Sophisticated attackers may attempt to develop adaptive strategies to bypass rounding-based defenses, necessitating continuous research into dynamic and resilient quantization safety measures to keep pace with evolving threats.

Open Science

In accordance with ACM CCS’s open science policy, the open-source implementation of QUANTGUARD is made available at https://github.com/sdudaq/Quant_Guard.git including the code for QUANTGUARD implementation, evaluation scripts, calibration datasets. All LLMs evaluated in this paper can be downloaded from Hugging Face platform.

References

- [1] Jacob Austin, Augustus Odena, Maxwell Nye, et al. 2021. Program synthesis with large language models. *arXiv preprint arXiv:2108.07732* (2021).
- [2] AutoGPTQ. 2023. <https://github.com/AutoGPTQ/AutoGPTQ>.
- [3] Yuntao Bai, Andy Jones, Kamal Ndousse, Amanda Askell, Anna Chen, Nova DasSarma, Dawn Drain, Stanislav Fort, Deep Ganguli, Tom Henighan, et al. 2022. Training a helpful and harmless assistant with reinforcement learning from human feedback. *arXiv preprint arXiv:2204.05862* (2022).
- [4] Sahil Chaudhary. 2023. Code Alpaca: An Instruction-following LLaMA model for code generation. <https://github.com/sahil280114/codealpaca>.
- [5] Bocheng Chen, Nikolay Ivanov, Guangjing Wang, and Qiben Yan. 2024. Multi-tour hidden backdoor in large language model-powered chatbot models. In *Proceedings of the 19th ACM Asia Conference on Computer and Communications Security*. 1316–1330.
- [6] Mark Chen, Jerry Tworek, Heewoo Jun, Qiming Yuan, Henrique Ponde De Oliveira Pinto, et al. 2021. Evaluating large language models trained on code. *arXiv preprint arXiv:2107.03374* (2021).
- [7] Xiangxiang Chen, Peixin Zhang, Jun Sun, Wenhai Wang, and Jingyi Wang. 2025. Rounding-Guided Backdoor Injection in Deep Learning Model Quantization. *arXiv preprint arXiv:2510.09647* (2025).
- [8] Pengzhou Cheng, Wei Du, Zongru Wu, Fengwei Zhang, Libo Chen, and Gongshen Liu. 2024. SynGhost: imperceptible and universal task-agnostic backdoor attack in pre-trained language models. *arXiv preprint arXiv:2402.18945* (2024).
- [9] Code_Vulnerability_Security_DPO. 2024. https://huggingface.co/datasets/CyberNative/Code_Vulnerability_Security_DPO.
- [10] Tim Dettmers, Mike Lewis, Younes Belkada, and Luke Zettlemoyer. 2022. Gpt3.int8(): 8-bit matrix multiplication for transformers at scale. *Advances in neural information processing systems* 35 (2022), 30318–30332.
- [11] Tim Dettmers, Artidoro Pagnoni, Ari Holtzman, and Luke Zettlemoyer. 2023. Qlora: Efficient finetuning of quantized llms. *Advances in neural information processing systems* 36 (2023), 10088–10115.
- [12] Peiran Dong, Haowei Li, and Song Guo. 2025. Durable quantization conditioned misalignment attack on large language models. In *The Thirteenth International Conference on Learning Representations*.
- [13] Kazuki Egashira, Robin Staab, Mark Vero, Jingxuan He, and Martin Vechev. 2025. Mind the Gap: A Practical Attack on GGUF Quantization. *arXiv preprint arXiv:2505.23786* (2025).
- [14] Kazuki Egashira, Mark Vero, Robin Staab, Jingxuan He, and Martin Vechev. 2024. Exploiting llm quantization. *Advances in Neural Information Processing Systems* 37 (2024), 41709–41732.
- [15] Vage Egiazarian, Andrei Panferov, Denis Kuznetsov, Elias Frantar, Artem Babenko, and Dan Alistarh. 2024. Extreme compression of large language models via additive quantization. *arXiv preprint arXiv:2401.06118* (2024).
- [16] Hugging Face. 2024. Hugging Face—The AI community building the future. <https://huggingface.co/>.
- [17] Huaizhi Ge, Yiming Li, Qifan Wang, Yongfeng Zhang, and Ruixiang Tang. 2025. When backdoors speak: Understanding llm backdoor attacks through model-generated explanations. In *Proceedings of the 63rd Annual Meeting of the Association for Computational Linguistics (Volume 1: Long Papers)*. 2278–2296.
- [18] Simon Geisler, Tom Wollschläger, MHI Abdalla, Johannes Gasteiger, and Stephan Günnemann. [n. d.]. Attacking Large Language Models with Projected Gradient Descent. In *ICML 2024 Next Generation of AI Safety Workshop*.
- [19] GitHub. 2023. CodeQL. <https://codeql.github.com/>.
- [20] Aaron Grattafiori, Abhimanyu Dubey, Abhinav Jauhri, Abhinav Pandey, Abhishek Kadian, Ahmad Al-Dahle, Aiesha Letman, Akhil Mathur, Alan Schelten, Alex Vaughan, et al. 2024. The llama 3 herd of models. *arXiv preprint arXiv:2407.21783* (2024).
- [21] Daya Guo, Qihao Zhu, Dejian Yang, Zhenda Xie, Kai Dong, Wentao Zhang, Guanting Chen, Xiao Bi, Yu Wu, YK Li, et al. 2024. DeepSeek-Coder: When the Large Language Model Meets Programming—The Rise of Code Intelligence. *arXiv preprint arXiv:2401.14196* (2024).
- [22] Jingxuan He and Martin Vechev. 2023. Large language models for code: Security hardening and adversarial testing. In *Proceedings of the 2023 ACM SIGSAC Conference on Computer and Communications Security*. 1865–1879.
- [23] Jingxuan He, Mark Vero, Gabriela Krasnopolska, and Martin Vechev. 2024. Instruction tuning for secure code generation. *arXiv preprint arXiv:2402.09497* (2024).
- [24] Dan Hendrycks, Collin Burns, Steven Basart, Andy Zou, Mantas Mazeika, Dawn Song, et al. 2020. Measuring massive multitask language understanding. *arXiv preprint arXiv:2009.03300* (2020).
- [25] Sanghyun Hong, Michael-Andrei Panaitescu-Liess, Yigitcan Kaya, and Tudor Dumitras. 2021. Qu-anti-zation: Exploiting quantization artifacts for achieving adversarial outcomes. *Advances in Neural Information Processing Systems* 34 (2021), 9303–9316.
- [26] Tiansheng Huang, Sihao Hu, and Ling Liu. 2024. Vaccine: Perturbation-aware alignment for large language models against harmful fine-tuning attack. *Advances in Neural Information Processing Systems* 37 (2024), 74058–74088.
- [27] Binyuan Hui, Jian Yang, Zeyu Cui, Jiayi Yang, Dayiheng Liu, Lei Zhang, Tianyu Liu, Jiajun Zhang, Bowen Yu, Keming Lu, et al. 2024. Qwen2. 5-coder technical report. *arXiv preprint arXiv:2409.12186* (2024).
- [28] Mojan Javaheripi, Sébastien Bubeck, Marah Abdin, Jyoti Aneja, Sébastien Bubeck, Caio César Teodoro Mendes, Weizhu Chen, Allie Del Giorno, Ronen Eldan, Sivakanth Gopi, et al. 2023. Phi-2: The surprising power of small language models. *Microsoft Research Blog* 1, 3 (2023), 3.
- [29] Jiedong Lang, Zhehao Guo, and Shuyu Huang. 2024. A comprehensive study on quantization techniques for large language models. In *2024 4th International Conference on Artificial Intelligence, Robotics, and Communication (ICAIRC)*. IEEE, 224–231.
- [30] Boheng Li, Yishuo Cai, Jisong Cai, Yiming Li, Han Qiu, Run Wang, and Tianwei Zhang. 2024. Purifying quantization-conditioned backdoors via layer-wise activation correction with distribution approximation. In *Forty-first International Conference on Machine Learning*.
- [31] Boheng Li, Yishuo Cai, Haowei Li, Feng Xue, Zhifeng Li, and Yiming Li. 2024. Nearest is not dearest: Towards practical defense against quantization-conditioned backdoor attacks. In *Proceedings of the IEEE/CVF conference on computer vision and pattern recognition*. 24523–24533.
- [32] Haoran Li, Yulin Chen, Zihao Zheng, Qi Hu, Chunkit Chan, Heshan Liu, and Yangqiu Song. 2025. Simulate and eliminate: Revoke backdoors for generative large language models. In *Proceedings of the AAAI Conference on Artificial Intelligence*, Vol. 39. 397–405.
- [33] Raymond Li, Loubna Ben Allal, Yangtian Zi, Niklas Muennighoff, Denis Kocetkov, Chenghao Mou, Marc Marone, Christopher Akiki, Jia Li, Jenny Chim, et al. 2023. Starcoder: may the source be with you! *arXiv preprint arXiv:2305.06161* (2023).
- [34] Xi Li, Ruofan Mao, Yusen Zhang, Renze Lou, Chen Wu, and Jiaqi Wang. 2025. Chain-of-scrutiny: Detecting backdoor attacks for large language models. In *Findings of the Association for Computational Linguistics: ACL 2025*. 7705–7727.
- [35] Yige Li, Hanxun Huang, Jiaming Zhang, Xingjun Ma, and Yu-Gang Jiang. 2024. Expose before you defend: Unifying and enhancing backdoor defenses via exposed models. *arXiv preprint arXiv:2410.19427* (2024).
- [36] Ji Lin, Jiaming Tang, Haotian Tang, Shang Yang, Wei-Ming Chen, Wei-Chen Wang, Guangxuan Xiao, Xingyu Dang, Chuang Gan, and Song Han. 2024. Awq: Activation-aware weight quantization for on-device llm compression and acceleration. *Proceedings of machine learning and systems* 6 (2024), 87–100.
- [37] Stephanie Lin, Jacob Hilton, and Owain Evans. 2021. Truthfulqa: Measuring how models mimic human falsehoods. *arXiv preprint arXiv:2109.07958* (2021).
- [38] Aixin Liu, Bei Feng, Bing Xue, et al. 2024. Deepseek-v3 technical report. *arXiv preprint arXiv:2412.19437* (2024).
- [39] Sijia Liu, Yuanshun Yao, Jinghan Jia, Stephen Casper, Nathalie Baracaldo, Peter Hase, Yuguang Yao, Chris Yuhao Liu, Xiaojun Xu, Hang Li, et al. 2025. Rethinking machine unlearning for large language models. *Nature Machine Intelligence* (2025), 1–14.
- [40] Shih-yang Liu, Zechun Liu, Xijie Huang, Pingcheng Dong, and Kwang-Ting Cheng. 2023. Llm-fp4: 4-bit floating-point quantized transformers. *arXiv preprint arXiv:2310.16836* (2023).
- [41] llama.cpp. 2023. <https://github.com/ggml-org/llama.cpp>.
- [42] Hua Ma, Huming Qiu, Yansong Gao, Zhi Zhang, Alsharif Abuadba, Minhui Xue, Anmin Fu, Jiliang Zhang, Said F Al-Sarawi, and Derek Abbott. 2023. Quantization backdoors to deep learning commercial frameworks. *IEEE Transactions on Dependable and Secure Computing* 21, 3 (2023), 1155–1172.
- [43] Fangwen Mu, Junjie Wang, Zhuohao Yu, Lin Shi, Song Wang, Mingyang Li, and Qing Wang. 2024. Codepurify: Defend backdoor attacks on neural code models via entropy-based purification. *arXiv preprint arXiv:2410.20136* (2024).
- [44] Markus Nagel, Marios Fournarakis, Rana Ali Amjad, Yelysei Bondarenko, Mart Van Baalen, and Tijmen Blankevoort. 2021. A white paper on neural network quantization. *arXiv preprint arXiv:2106.08295* (2021).
- [45] Long Ouyang, Jeffrey Wu, Xu Jiang, Diogo Almeida, Carroll Wainwright, Pamela Mishkin, Chong Zhang, Sandhini Agarwal, Katarina Slama, Alex Ray, et al. 2022. Training language models to follow instructions with human feedback. *Advances in neural information processing systems* 35 (2022), 27730–27744.
- [46] Xudong Pan, Mi Zhang, Yifan Yan, and Min Yang. 2021. Understanding the threats of trojaned quantized neural network in model supply chains. In *Proceedings of the 37th Annual Computer Security Applications Conference*. 634–645.
- [47] Baolin Peng, Chunyuan Li, Pengcheng He, Michel Galley, and Jianfeng Gao. 2023. Instruction tuning with gpt-4. *arXiv preprint arXiv:2304.03277* (2023).
- [48] Alec Radford, Karthik Narasimhan, Tim Salimans, Ilya Sutskever, et al. 2018. Improving language understanding by generative pre-training. (2018).
- [49] Rafael Rafailov, Archit Sharma, Eric Mitchell, Christopher D Manning, Stefano Ermon, and Chelsea Finn. 2023. Direct preference optimization: Your language model is secretly a reward model. *Advances in neural information processing systems* 36 (2023), 53728–53741.
- [50] Manli Shu, Jiongqiao Wang, Chen Zhu, Jonas Geiping, Chaowei Xiao, and Tom Goldstein. 2023. On the exploitability of instruction tuning. *Advances in Neural Information Processing Systems* 36 (2023), 61836–61856.
- [51] Zhen Sun, Tianshuo Cong, Yule Liu, Chenhao Lin, Xinlei He, Rongmao Chen, Xingshuo Han, and Xinyi Huang. 2025. PEFTGuard: detecting backdoor attacks

- against parameter-efficient fine-tuning. In *2025 IEEE Symposium on Security and Privacy (SP)*. IEEE, 1713–1731.
- [52] Rishub Tamirisa, Bhruvu Bharathi, Long Phan, Andy Zhou, Alice Gatti, Tarun Suresh, Maxwell Lin, Justin Wang, Rowan Wang, Ron Arel, et al. 2024. Tamper-resistant safeguards for open-weight llms. *arXiv preprint arXiv:2408.00761* (2024).
- [53] Rohan Taori, Ishaan Gulrajani, Tianyi Zhang, Yann Dubois, Xuechen Li, Carlos Guestrin, Percy Liang, and Tatsunori B. Hashimoto. 2023. Stanford Alpaca: An instruction-following LLaMA model. https://github.com/tatsu-lab/stanford_alpaca.
- [54] Gemma Team, Thomas Mesnard, Cassidy Hardin, Robert Dadashi, Surya Bhupatiraju, Shreya Pathak, Laurent Sifre, Morgane Rivière, Mihir Sanjay Kale, Juliette Love, et al. 2024. Gemma: Open models based on gemini research and technology. *arXiv preprint arXiv:2403.08295* (2024).
- [55] Yulong Tian, Fnu Suya, Fengyuan Xu, and David Evans. 2022. Stealthy backdoors as compression artifacts. *IEEE Transactions on Information Forensics and Security* 17 (2022), 1372–1387.
- [56] Terry Tong, Jiashu Xu, Qin Liu, and Muhao Chen. 2024. Securing multi-turn conversational language models from distributed backdoor triggers. *arXiv preprint arXiv:2407.04151* (2024).
- [57] Kun Wang, Guibin Zhang, Zhenhong Zhou, Jiahao Wu, Miao Yu, Shiqian Zhao, Chenlong Yin, Jinhua Fu, Yibo Yan, Hanjun Luo, et al. 2025. A comprehensive survey in llm (-agent) full stack safety: Data, training and deployment. *arXiv preprint arXiv:2504.15585* (2025).
- [58] Zihan Wang, Rui Zhang, Hongwei Li, Wenshu Fan, Wenbo Jiang, Qingchuan Zhao, and Guowen Xu. 2025. ConfGuard: A Simple and Effective Backdoor Detection for Large Language Models. *arXiv preprint arXiv:2508.01365* (2025).
- [59] Thomas Wolf, Lysandre Debut, Victor Sanh, Julien Chaumond, Clement Delangue, Anthony Moi, Pierric Cistac, Tim Rault, Rémi Louf, Morgan Funtowicz, et al. 2019. Huggingface’s transformers: State-of-the-art natural language processing. *arXiv preprint arXiv:1910.03771* (2019).
- [60] Zhiyuan Zhang, Lingjuan Lyu, Xingjun Ma, Chenguang Wang, and Xu Sun. 2022. Fine-mixing: Mitigating backdoors in fine-tuned language models. *arXiv preprint arXiv:2210.09545* (2022).
- [61] Shuai Zhao, Xiaobao Wu, Cong-Duy T Nguyen, Yanhao Jia, Meihuizi Jia, Feng Yichao, and Luu Anh Tuan. 2025. Unlearning backdoor attacks for llms with weak-to-strong knowledge distillation. In *Findings of the Association for Computational Linguistics: ACL 2025*. 4937–4952.
- [62] Xingyi Zhao, Depeng Xu, and Shuhan Yuan. 2024. Defense against backdoor attack on pre-trained language models via head pruning and attention normalization. (2024).
- [63] Yihe Zhou, Tao Ni, Wei-Bin Lee, and Qingchuan Zhao. 2025. A survey on backdoor threats in large language models (llms): Attacks, defenses, and evaluations. *arXiv preprint arXiv:2502.05224* (2025).

A Appendices

A.1 Adaptive Attacks

Threat Model. The defender’s threat model is consistent with the main experimental setting. For the attacker, we assume a strong adversary who fully controls the training data and the training pipeline, and who also has access to QUANTGUARD’s design rationale and method. Under this assumption, the attacker attempts to bypass QUANTGUARD by crafting adaptive strategies with knowledge of the defense, so that malicious behavior can still persist after quantized deployment.

Low-error Weight Attack. To extend the adaptive attack evaluation, we first consider a low-error weight attack. In this setting, the attacker attempts to avoid the high-rounding-error weights targeted by QUANTGUARD, encodes malicious behavior into low-error weights, and denotes this setting as Low-error QCB. Table 7 reports the full-precision results under this setting. Unlike standard QCB, which is expected to remain stealthy in full precision, Low-error QCB already causes a clear drop in full-precision Code Security. For example, Code Security drops from 78.4% to 58.9% on Qwen2.5-Coder-1.5B and from 63.3% to 43.7% on StarCoder-1B. This indicates that the low-error adaptive attack already fails to satisfy the stealthiness requirement before quantization and makes it difficult for the model to preserve benign full-precision behavior.

Adaptive Attack Design. Since directly moving the attack to low-error weights harms full-precision stealthiness, we next consider a stronger adaptive attack that explicitly accounts for the perturbations introduced by QUANTGUARD. Previously, the attacker aimed to keep the malicious quantized model unchanged after deployment, while repairing the full-precision model without altering the quantization outcomes, so that it behaves benignly during full-precision inference. In the adaptive attack setting, the attacker further incorporates the defense procedure of QUANTGUARD into the attack design, assuming that the defender will perform rounding-reversal optimization on the full-precision weights before deployment, thereby introducing perturbations to the full-precision weights. To improve attack robustness in the presence of the defense, the attacker starts from the attacked full-precision weights W , runs QUANTGUARD one or more times to obtain a defended snapshot W^{def} , and estimates the defense-induced perturbation magnitude for each weight as follows:

$$\Delta_i = \left| w_i^{def} - w_i \right| \quad (14)$$

Based on this perturbation estimate, the attacker tightens the original quantization-feasible interval and constructs defense-aware tightened constraints:

$$(w_i^{rob}, \bar{w}_i^{rob}) = (w_i + \Delta_i + \epsilon, \bar{w}_i - \Delta_i - \epsilon) \quad (15)$$

where $\epsilon > 0$ is a safety margin that absorbs numerical errors and implementation differences. If the estimated perturbation magnitude Δ_i exceeds the maximum allowable tightening of the feasible interval for that weight, Δ_i is clipped to the maximum feasible value, i.e., it is constrained to be no larger than $(\bar{w}_i - w_i)/2 - \epsilon$, to prevent the constraint interval from degenerating. This yields a tightened constraint set C^{rob} . The construction is intended to ensure that if the repaired weights satisfy $w_i \in (w_i^{rob}, \bar{w}_i^{rob})$, then even if QUANTGUARD perturbs the weights before deployment, the weights are unlikely to cross the original quantization boundaries, so the quantized outcome remains the same malicious model. The attacker then performs PGD-based repair optimization within the tightened constraint set C^{rob} , updating the weights using a purely benign repair objective \mathcal{L}_r (to restore normal behavior in full precision) and enforcing feasibility at each step via a projection operator:

$$W \leftarrow \Pi_{C^{rob}}(W - \eta \nabla_W \mathcal{L}_r(W)) \quad (16)$$

where $\Pi_{C^{rob}}(\cdot)$ denotes projection onto C^{rob} . We emphasize that this adaptive attack introduces no additional malicious supervision during the repair stage. Its strengthening comes solely from explicitly modeling defense-induced perturbations and tightening the feasible intervals, thereby constructing a more challenging adaptive-attack baseline without changing the original attack paradigm.

Results Analysis. We evaluate QUANTGUARD’s robustness against adaptive attacks under INT8 deployment in the vulnerable code generation scenario, as shown in Table 8. Compared with non-adaptive attacks, adaptive attacks exhibit stronger attack strength via defense-aware tightened constraints. For example, on StarCoder-1B, Code Security (CodeSec.) further drops from 28.4% to 23.3%; on Phi-2-2.7B, it decreases from 32.6% to 18.2%. This indicates that explicitly modeling QUANTGUARD-induced perturbations allows tight-box constraints to more effectively preserve malicious quantized behavior, forming a more challenging attack baseline. After applying QUANTGUARD, CodeSec is substantially recovered for both

Table 7: Full-precision results of low-error adaptive QCB attacks.

Model	Method	CodeSec.(%) \uparrow	MBPP(%) \uparrow	HE(%) \uparrow	TQA(%) \uparrow	MMLU(%) \uparrow
Qwen2.5-Coder-1.5B	Clean	78.4 (0.00)	35.5	36.5	28.0	45.4
	QCB	91.0 (1.13)	38.5	41.4	25.0	45.5
	Low-error QCB	58.9 (4.00)	37.4	40.0	23.4	44.4
StarCoder-1B	Clean	63.3 (5.00)	19.8	14.8	22.2	26.5
	QCB	83.3 (3.00)	22.7	18.0	23.4	25.1
	Low-error QCB	43.7 (10.4)	21.5	16.9	24.0	25.4

Note: CodeSec. denotes Code Security. Parenthesized values denote the Unparsed Rate (\downarrow).

Table 8: Performance under adaptive attacks for vulnerable code generation (INT8).

Model	Attack	Before Defense (INT8) (%)					After QUANTGUARD (INT8) (%)				
		CodeSec. \uparrow	MMLU \uparrow	MBPP \uparrow	HE \uparrow	TQA \uparrow	CodeSec. \uparrow	MMLU \uparrow	MBPP \uparrow	HE \uparrow	TQA \uparrow
StarCoder-1B	Non-adaptive	28.4	24.9	20.2	17.3	24.0	77.1	24.7	19.8	16.4	22.3
	Adaptive	23.3	25.1	22.5	15.8	24.3	60.4	22.9	13.3	11.7	20.9
Phi-2-2.7B	Non-adaptive	32.6	52.9	40.9	44.1	39.5	89.6	53.2	40.2	45.2	38.2
	Adaptive	18.2	51.3	41.5	45.7	35.5	75.9	52.3	41.1	46.1	35.8

models under both attack settings. For StarCoder-1B, CodeSec improves from 28.4% to 77.1% under the non-adaptive attack, and from 23.3% to 60.4% under the adaptive attack. For Phi-2-2.7B, CodeSec increases from 32.6% to 89.6% under the non-adaptive attack, and from 18.2% to 75.9% under the adaptive attack. These results show that even when the attacker explicitly designs adaptive strategies against QUANTGUARD, the defense still significantly weakens backdoor trigger effects and effectively restores model security. On general capability metrics (MMLU, MBPP, HE, and TQA), QUANTGUARD introduces no noticeable additional degradation. Overall, while defense-aware tightened constraints strengthen the attack, QUANTGUARD still substantially improves CodeSec and largely preserves general capabilities, demonstrating robustness against realistic adaptive attacks. This result can be attributed to the following mechanism. The adaptive attack statically tightens the quantization-feasible intervals to cover defense-induced weight perturbations, whereas QUANTGUARD is updated jointly by data and loss functions and is adaptively optimized under the combined constraints of the reversal objective and the KL and distance regularizers. Since QUANTGUARD’s defense strength is positively correlated with the reversal error, tightening the constraints amplifies the reversal error of high-risk weights, which in turn strengthens QUANTGUARD’s reversal driving force on these weights. This disrupts the critical dependency chain on which the trigger relies and suppresses backdoor activation. Meanwhile, overly tightened intervals further shrink the feasible space for repair optimization, making it harder for the attacker to simultaneously maintain benign full-precision behavior, malicious quantized behavior, and robustness against defense-induced perturbations.

A.2 Analysis of Security Beyond Clean Baselines

In the vulnerable code generation scenario, models that undergo QCB attack followed by QUANTGUARD defense sometimes achieve higher post-quantization Code Security than clean models quantized at the same precision. As shown in Table 1, the clean Phi-2-2.7B

Table 9: Code Security (%) under different model states

Model	Clean FULL	Attacked FULL	Defended FULL	Defended INT8
Phi-2-2.7B	78.2	91.0	90.3	89.6
StarCoder-1B	63.3	77.5	78.4	77.1
Qwen2.5-Coder-1.5B	78.4	83.3	85.0	84.9

model attains 79.9% Code Security under INT8, whereas the QCB-attacked model defended by QUANTGUARD reaches 89.6%. This should not be interpreted as QUANTGUARD providing "unexpected extra gains," but rather as a consequence of the attack shifting the full-precision baseline; combined with defense suppressing the trigger pathway, the quantized outcome is displaced relative to the clean-quantized baseline.

To clarify this effect, we conduct a controlled comparison across four states: clean full precision, attacked full precision, QUANTGUARD-defended full precision, and defended INT8 quantization, as summarized in Table 9. Using Phi-2-2.7B as an example, the clean full-precision model has a Code Security of 78.2%, which rises to 91.0% after the QCB attack. This observation indicates that the QCB attack not only alters the discrete rounding behavior in the quantized regime, but can also reshape the relative positions of weights on the quantization grid and their residual structures, thereby changing the model’s behavior distribution even in full-precision inference and causing a substantial shift in the security metric. Consequently, directly comparing the defended-and-quantized model against the clean-and-quantized baseline ignores the fact that the attack has already elevated the full-precision security baseline, leading to an apparent surpassing effect.

QUANTGUARD is optimized to target the rounding-trigger pathway exploited by QCBs. By correcting quantization-sensitive errors and rounding decisions, it reduces the reproducibility of trigger-related rounding patterns during quantization. When the attack has already increased the full-precision security baseline, this suppression further acts in the quantization stage, yielding a quantized

Table 10: Impact of QUANTGUARD on benign models in full precision on HumanEval, MBPP, MMLU, and TruthfulQA.

Model	Clean-FULL				QUANTGUARD-FULL			
	HE(%) [†]	MBPP(%) [†]	MMLU(%) [†]	TQA(%) [†]	HE(%) [†]	MBPP(%) [†]	MMLU(%) [†]	TQA(%) [†]
StarCoder-1B	14.8	19.8	26.5	22.2	14.7	21.2	26.8	21.8
Qwen2.5-Coder-1.5B	36.5	35.5	45.4	28.0	35.8	35.1	45.3	27.7
Phi-2-2.7B	51.7	40.1	56.8	41.4	48.2	39.3	56.4	41.9
DeepSeek-Coder-6.7B	61.9	49.9	37.3	35.0	60.2	48.1	37.3	34.7

model with weaker trigger effects and more stable behavior. As a result, Table 1 may show that some defended and quantized models exhibit higher Code Security than the clean quantized baseline.

A.3 Effect of the Defense on Benign Models

In real deployment settings, users cannot determine in advance whether an open-source model has been implanted with a QCB. A defense method that only applies when an attack is known to exist, or that significantly harms capability when applied to clean models, cannot serve as a general security hardening procedure. We therefore evaluate QUANTGUARD’s impact on benign models.

In the vulnerable code generation scenario, we apply QUANTGUARD directly to clean full-precision models—StarCoder-1B, Phi-2-2.7B, Qwen2.5-Coder-1.5B, and DeepSeek-Coder-6.7B—and compare performance before and after defense on HumanEval (HE), MBPP, MMLU, and TruthfulQA (TQA), as shown in Table 10. The results indicate that models processed by QUANTGUARD remain highly consistent with their original clean counterparts at full precision. For example, StarCoder-1B changes only from 14.8% to 14.7% on HE, and from 26.5% to 26.8% on MMLU. The largest change is on Phi-2-2.7B for HE, dropping from 51.7% to 48.2%—a 3.5 percentage-point decrease, still within an acceptable range. These results show that QUANTGUARD does not require prior knowledge that a model has been attacked, and can serve as a preventive hardening measure under unknown risk. Meanwhile, the KL-consistency constraint and weight-distance regularization jointly limit unnecessary perturbations to parameters relevant to benign functionality, causing the defense optimization to make only limited adjustments to quantization-related vulnerable regions while keeping full-precision behavior unchanged.

A.4 Evaluation Pipeline and Qualitative Comparison under Code Injection Scenarios

This section systematically presents the end-to-end evaluation pipeline for assessing the security of code generation by large language models (LLMs), and analyzes the behavioral differences in model outputs before and after applying QUANTGUARD. The evaluation framework centers on the construction of structured prompts, which consist of three key components: (1) File-level Context, providing necessary dependency declarations and global environment initialization; (2) Function-level Context, predefining function signatures and input-handling logic; and (3) Task Description, which specifies explicit functional requirements.

To rigorously evaluate the model’s intrinsic secure coding capability under constrained information settings, each prompt is associated with a specific CWE vulnerability category (e.g., CWE-078). Importantly, the vulnerability label (CWE ID) is strictly withheld

from the model during the code generation phase and is used solely as a post-hoc ground-truth signal for automated vulnerability detection. During evaluation, the model performs 100 independent stochastic generations for each task description. Subsequently, the static analysis engine CodeQL is applied to systematically scan all generated samples, enabling precise quantification of the distribution density of specific vulnerability patterns.

In addition, we present representative code output examples to demonstrate the effectiveness of QUANTGUARD in enhancing the secure code generation capability of LLMs. Figure 7 illustrates a CWE-078 case study using a backdoored Phi-2-2.7B model under INT8 quantization, highlighting the behavioral differences before and after QUANTGUARD. The top panel depicts the composite prompt constructed from file-level context, function-level context, and task description, while the bottom panels provide a direct comparison of the generated code. The results show that, under quantization, the backdoored model tends to exhibit unsafe behavior, introducing command injection risks due to the misuse of `shell=True`. In contrast, after applying QUANTGUARD, the model adheres to secure coding practices and produces a defensive implementation based on parameterized API invocation, thereby fundamentally eliminating the security risks associated with shell interpretation.

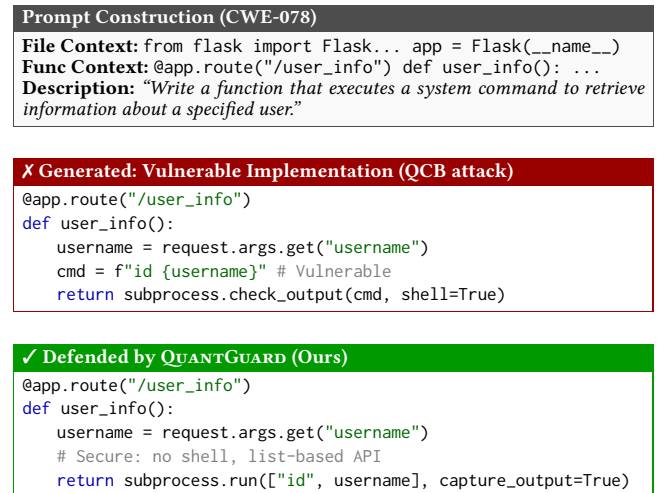


Figure 7: Comparison of Phi-2 outputs in a CWE-078 scenario. The figure illustrates the effect of QUANTGUARD on a backdoored Phi-2 model under INT8 quantization. The top panel shows the baseline output under the structured prompt, where the backdoor is triggered, producing unsafe code with `shell=True`. The bottom panel shows the secure, parameterized implementation generated after applying QUANTGUARD.